

AD-A058 382

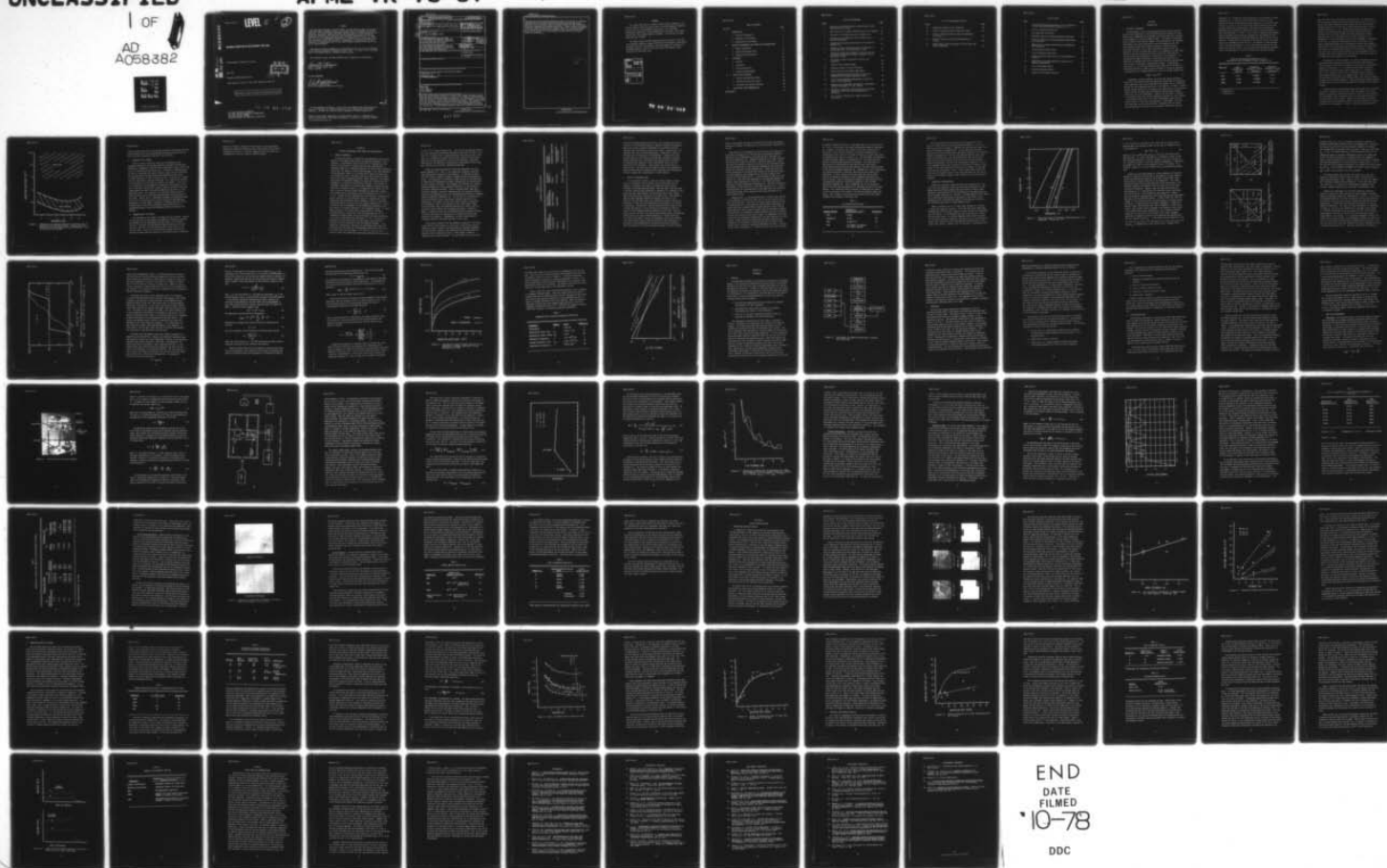
AIR FORCE MATERIALS LAB WRIGHT-PATTERSON AFB OHIO
INFRARED ABSORPTION IN ZINC SELENIDE THIN FILMS.(U)
MAY 78 D F O'BRIEN
AFML-TR-78-37

F/G 20/5

UNCLASSIFIED

1 OF
AD
A058382

NL



AFML-TR-78-37

LEVEL

II

2

ADA 058382

AU NO. _____
DDC FILE COPY

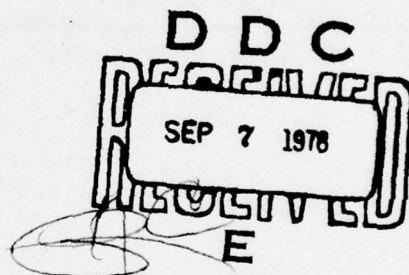
INFRARED ABSORPTION IN ZINC SELENIDE THIN FILMS

Electromagnetic Materials Division

May 1978

TECHNICAL REPORT AFML-TR-78-37

Final Report for Period 1 July 1974 through 30 June 1977



Approved for public release; distribution unlimited.

78 08 24 003

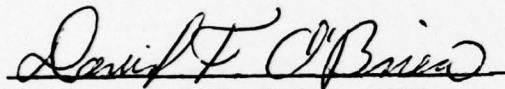
AIR FORCE MATERIALS LABORATORY
AIR FORCE WRIGHT AERONAUTICAL LABORATORIES
AIR FORCE SYSTEMS COMMAND
WRIGHT-PATTERSON AIR FORCE BASE, OHIO 45433

NOTICE

When Government drawings, specifications, or other data are used for any purpose other than in connection with a definitely related Government procurement operation, the United States Government thereby incurs no responsibility nor any obligation whatsoever; and the fact that the government may have formulated, furnished, or in any way supplied the said drawings, specifications, or other data, is not to be regarded by implication or otherwise as in any manner licensing the holder or any other person or corporation, or conveying any rights or permission to manufacture, use, or sell any patented invention that may in any way be related thereto.

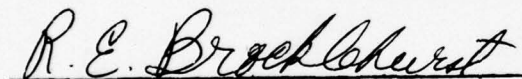
This report has been reviewed by the Information Office (OI) and is releasable to the National Technical Information Service (NTIS). At NTIS, it will be available to the general public, including foreign nations.

This technical report has been reviewed and is approved for publication.



DAVID F. O'BRIEN, Major, USAF
Project Engineer

FOR THE COMMANDER



MR. ROBERT E. BROCKLEHURST
Chief, Electromagnetic Materials Division

"If your address has changed, if you wish to be removed from our mailing list, or if the addressee is no longer employed by your organization please notify AFML/LP, W-PAFB, OH 45433 to help us maintain a current mailing list".

Copies of this report should not be returned unless return is required by security considerations, contractual obligations, or notice on a specific document.

UNCLASSIFIED

SECURITY CLASSIFICATION OF THIS PAGE (When Data Entered)

REPORT DOCUMENTATION PAGE		READ INSTRUCTIONS BEFORE COMPLETING FORM	
1. REPORT NUMBER AFML-TR-78-37	2. GOVT ACCESSION NO.	3. RECIPIENT'S CATALOG NUMBER	
4. TITLE (and Subtitle) INFRARED ABSORPTION IN ZINC SELENIDE THIN FILMS		5. TYPE OF REPORT & PERIOD COVERED Final Report for period 1 Jul 74 to 30 Jun 75	
6. PERFORMING ORG. REPORT NUMBER		7. CONTRACT OR GRANT NUMBER(s)	
8. AUTHOR(s) David F. O'Brien, Major, USAF		9. PROGRAM ELEMENT, PROJECT, TASK AREA & WORK UNIT NUMBERS Project 7367 Task 736703	
10. PERFORMING ORGANIZATION NAME AND ADDRESS Air Force Materials Laboratory (AFML/LPO) Air Force Wright Aeronautical Laboratories Wright-Patterson AFB, Ohio 45433		11. REPORT DATE May 1978	
12. CONTROLLING OFFICE NAME AND ADDRESS Air Force Materials Laboratory (AFML/LPO) Air Force Wright Aeronautical Laboratories Wright-Patterson AFB, Ohio 45433		13. NUMBER OF PAGES 91	
14. MONITORING AGENCY NAME & ADDRESS (if different from Controlling Office)		15. SECURITY CLASS. (of this report) Unclassified	
16. DISTRIBUTION STATEMENT (of this Report)		15a. DECLASSIFICATION/DOWNGRADING SCHEDULE	
17. DISTRIBUTION STATEMENT (of the abstract entered in Block 20, if different from Report) Approved for public release; distribution unlimited. (12) 92 p.			
18. SUPPLEMENTARY NOTES			
19. KEY WORDS (Continue on reverse side if necessary and identify by block number) Absorption Thin Films II-VI Compounds Zinc Selenide			
20. ABSTRACT (Continue on reverse side if necessary and identify by block number) Low loss antireflection coatings for infrared laser windows have been found to have absorption coefficients which are three to four orders of magnitude higher than was predicted from bulk material properties. An investigation of the causes for this increase in zinc selenide coatings was performed. Prior growth studies and theoretical descriptions of the thin film growth process indicated that variations in stoichiometry might be a cause for the high absorption measured in the coatings. An experimental program in which zinc selenide coatings were			

DD FORM 1 JAN 73 1473 EDITION OF 1 NOV 65 IS OBSOLETE

UNCLASSIFIED

SECURITY CLASSIFICATION OF THIS PAGE (When Data Entered)

012 320

elt

UNCLASSIFIED

SECURITY CLASSIFICATION OF THIS PAGE(When Data Entered)

N deposited onto calcium fluoride substrates under a wide variety of conditions revealed that the infrared absorption of the coatings decreased as the deposition rate was lowered. This correlated directly with the theoretical predictions based upon stoichiometry variations. Several surface and chemical techniques indicated that the most probable cause for the abnormal absorption in zinc selenide thin films was an increase in the zinc to selenium ratio which could be controlled to some extent by proper selection of vacuum deposition conditions. ↗

UNCLASSIFIED

SECURITY CLASSIFICATION OF THIS PAGE(When Data Entered)

FOREWORD

This report describes an in-house research effort conducted in the Laser and Optical Materials Branch (LPO) of the Electromagnetic Materials Division (LP), Air Force Materials Laboratory, Air Force Wright Aeronautical Laboratories, Wright-Patterson Air Force Base, Ohio, under Project 7367, Task 736703, Work Unit 73670315. The work was initiated under Work Unit 73670314. ✓

The report covers all work conducted during the period 1 July 1974 to 31 December 1976 and is based on portions of the author's dissertation submitted in partial fulfillment of the requirements for the Doctor of Philosophy degree at the Air Force Institute of Technology, Wright-Patterson Air Force Base, Ohio.

ABSTRACTED BY	
NRW	Write Section <input checked="" type="checkbox"/>
DDC	Ref Section <input type="checkbox"/>
UNANNOUNCED	<input type="checkbox"/>
JUSTIFICATION.....	
BY.....	
DISTRIBUTION/AVAILABILITY CODES	
DTIC	AVAIL. and/or SPECIAL
A	

78 08 24 003

TABLE OF CONTENTS

SECTION	PAGE
I INTRODUCTION	1
1. Historical Background	1
2. Statement of the Problem	5
3. Organization of the Report	5
II PREVIOUS EXPERIMENTAL AND THEORETICAL CONSIDERATIONS	7
1. General Background	7
2. Related Experimental Work	10
3. Theoretical Considerations	13
III EXPERIMENT	25
1. Overview	25
2. Substrates	27
3. Coating Depositions	29
4. Analytical Measurements	31
IV RESULTS AND DISCUSSION	53
1. Surface and Interface Effects	53
2. Absorption Within the Coating	60
3. Structural and Chemical Analysis	68
V CONCLUSIONS AND RECOMMENDATIONS	76
BIBLIOGRAPHY	79

LIST OF ILLUSTRATIONS

FIGURE		PAGE
1	Comparison of Infrared Absorption Coefficients of Bulk ZnSe and ZnSe Thin Films	4
2	Vapor Pressures of Elements Comprising the II-VI Compounds	14
3	Variation in Film Composition with Incident Flux	16
4	Variation in Film Composition with Incident Flux at Elevated Temperature	16
5	Composition of Condensed CdSe Layers as a Function of Incident Flux	18
6	Theoretical Excess Volume Fraction of Zn Required to Produce Observed $1.06 \mu\text{m}$ Absorption in ZnSe	22
7	Theoretical Relationship Between Zn Particle Size and Concentration Required to Produce Increased $1.06 \mu\text{m}$ Absorption in ZnSe	24
8	Flow Chart of Sample Preparation, Coating, and Evaluation	26
9	Interior View of Vacuum Chamber	32
10	Schematic Diagram of Laser Calorimeter	34
11	Output from Laser Calorimetry Measurement	37
12	Normalized Absorption Coefficient of a Thin Film Computed With and Without Coherence Effects	39
13	Typical Spectrophotometer Measurement of ZnSe Thin Film on a CaF_2 Substrate	43
14	Comparison of Conventional and Nomarski Interference Contrast Micrographs of a CaF_2 Surface	48
15	Variation of Substrate Surface Features and Infrared Absorption Coefficient After Repeated Optical Polishing	55
16	$10.6 \mu\text{m}$ Optical Absorption vs Sample Length for a KCl Crystal	57

LIST OF ILLUSTRATIONS (CONT'D)

FIGURE		PAGE
17	Absorption Change with Film Thickness	58
18	Effect of Deposition Rate on Refractive Index	65
19	Effect of Deposition Rate on ZnSe Film Absorption at 1.06 μm	67
20	Effect of Excess Se on ZnSe Film Absorption at 1.06 μm	69
21	Auger Electron Profile Analyses of ZnSe on Glass and Al Foil Substrates	74

LIST OF TABLES

TABLE		PAGE
1	Predicted and Measured Absorption of 10.6 μm Radiation in Thin Films Having Optical Thickness of $\lambda/4$	2
2	Extrinsic Absorption Mechanisms	9
3	ZnSe Absorption Coefficient	12
4	Parameters Used to Calculate Absorption Coefficient	23
5	Effect of Absorption on Spectrophotometer Measurement of a Thin Film	45
6	Comparison of Thickness and Refractive Index Measurement Techniques	46
7	Surface Analysis Sensitivities	50
8	X-ray Fluorescence Sensitivity	51
9	Thermal Expansion Coefficients of Infrared Materials at 300°K	61
10	Comparisons of Coatings Deposited at High and Low Substrate Temperatures	62
11	X-ray Fluorescence Results	71
12	Electron Microprobe Results	71
13	Summary of Stoichiometry Analyses	75

SECTION 1

INTRODUCTION

1. HISTORICAL BACKGROUND

The development of thin film technology and specifically the application of this technology to providing antireflective coatings for transparent optical components has progressed to the point where such coatings can be produced on a routine production basis. The advent of high power (multi-kilowatt) laser systems, however, has caused new and more demanding requirements to be placed upon both the optical components used with these systems and upon the reflective and antireflective coatings associated with them. One of these requirements specifies that the absorption of laser radiation which occurs in a component as a beam passes through it must be kept below the level at which the resulting heat build-up could cause degradation or destruction of the component. This requirement has made consideration of the absorption coefficient of materials an important part of the procedure for selecting component materials for use in high power infrared laser systems. The absorption coefficient, β , is a material parameter which specifies the decrease in transmitted intensity or power (P) with distance (x) caused by absorption or scattering and is commonly defined by its use in the Beer-Lambert Law

$$P(x) = P_0 e^{-\beta x} \quad (1)$$

Heretofore, coatings designers had justifiably ignored absorption within thin film coatings since the absorption coefficients of transparent coating materials were usually negligible and, perhaps just as significant, because the films themselves were only on the order of 1 μ m thick. For the optical systems which were in existence, this combination of low absorption coefficient and extremely short pathlength caused any power absorbed within the film to be immeasurable. However, for the drastic increases in transmitted power that could be reasonably projected for laser systems, it soon became evident that this formerly immeasurable quantity could readily attain an intolerably high magnitude. Nevertheless, even when very high power levels were considered, it appeared that for certain selected materials the factors of low absorption coefficient and short

pathlength still allowed the coating absorption to be neglected in design considerations. In the early 1970's, when the Air Force initiated programs to develop antireflection coated windows for use with high power, 10.6 μm CO_2 lasers, it was discovered that these assumptions were wrong and that state-of-the-art absorption coefficients for coatings were anomalously and significantly higher than those of the same materials in bulk form (Reference 1). Table 1 lists results of absorption measurements made on candidate infrared coatings together with the absorption value that had been predicted based upon the absorption coefficient of the bulk material. The absorption is expressed as the percent loss of laser beam power due to absorption within the film. The materials listed represent some of the best candidates for use as antireflection coatings for high power laser windows, and yet, as can be seen from the measured absorption losses, the absorption in a thin film coating can comprise the major

TABLE 1

PREDICTED AND MEASURED ABSORPTION OF 10.6 μm
RADIATION IN THIN FILMS HAVING OPTICAL THICKNESS OF $\lambda/4$

Material	Bulk Absorption (cm^{-1}) *	Predicted Absorption Loss (Percent)	Measured Absorption Loss (Percent) **
ZnS	0.15	0.0019	0.18
ZnSe	0.004	0.00004	0.12
CdTe	0.001	0.00001	0.19

* (Reference 2)

** (Reference 3)

source of power loss in the entire window structure. The importance of this problem was recognized early and prompted the Air Force to initiate several development programs directed toward improving the absorption characteristics of thin films used as antireflection coatings for laser windows (References 2, 3, 4). These programs improved coating technology to a point where state-of-the-art multilayer antireflection coatings for 10.6 μm laser systems can now be created which display absorption levels of 0.05 percent for an optical thickness of $\lambda/2$ (Reference 5). Since there was initially little knowledge or experience in the "art" of producing low absorption films, a great part of this order of magnitude decrease in film absorption resulted from systematic modification of the vacuum deposition conditions to the point where they were found to be optimized with respect to film absorption. However, since there was a time constraint under which the improvements had to be achieved, very little in-depth study was made of the detailed causes for the anomalously high absorption in the coatings.

Simultaneously with the programs for coatings improvement, parallel efforts were being conducted to improve some of these same materials (CdTe and ZnSe) in bulk form with respect to both optical and mechanical properties (References 6, 7). Although the bulk optical absorption coefficients of these materials were already low, as is indicated in Table 1, the theoretical lower limit of absorption due to intrinsic (multiphonon) processes was still somewhat lower. Thus, efforts were directed toward identifying and eliminating some of the extrinsic sources of absorption in the bulk materials. These more detailed studies provided valuable input to the thin film investigations conducted in this research program.

Although progress has been made toward lowering both bulk and coating absorption in materials such as ZnSe, a wide discrepancy still exists between the absorption coefficient measured in each form of the material. This discrepancy is not limited to the 10.6 μm wavelength where most of the past data has been obtained. Rather, the same trend is observed throughout the entire wavelength region in which the material is normally considered to be transparent. Figure 1 summarizes data obtained from

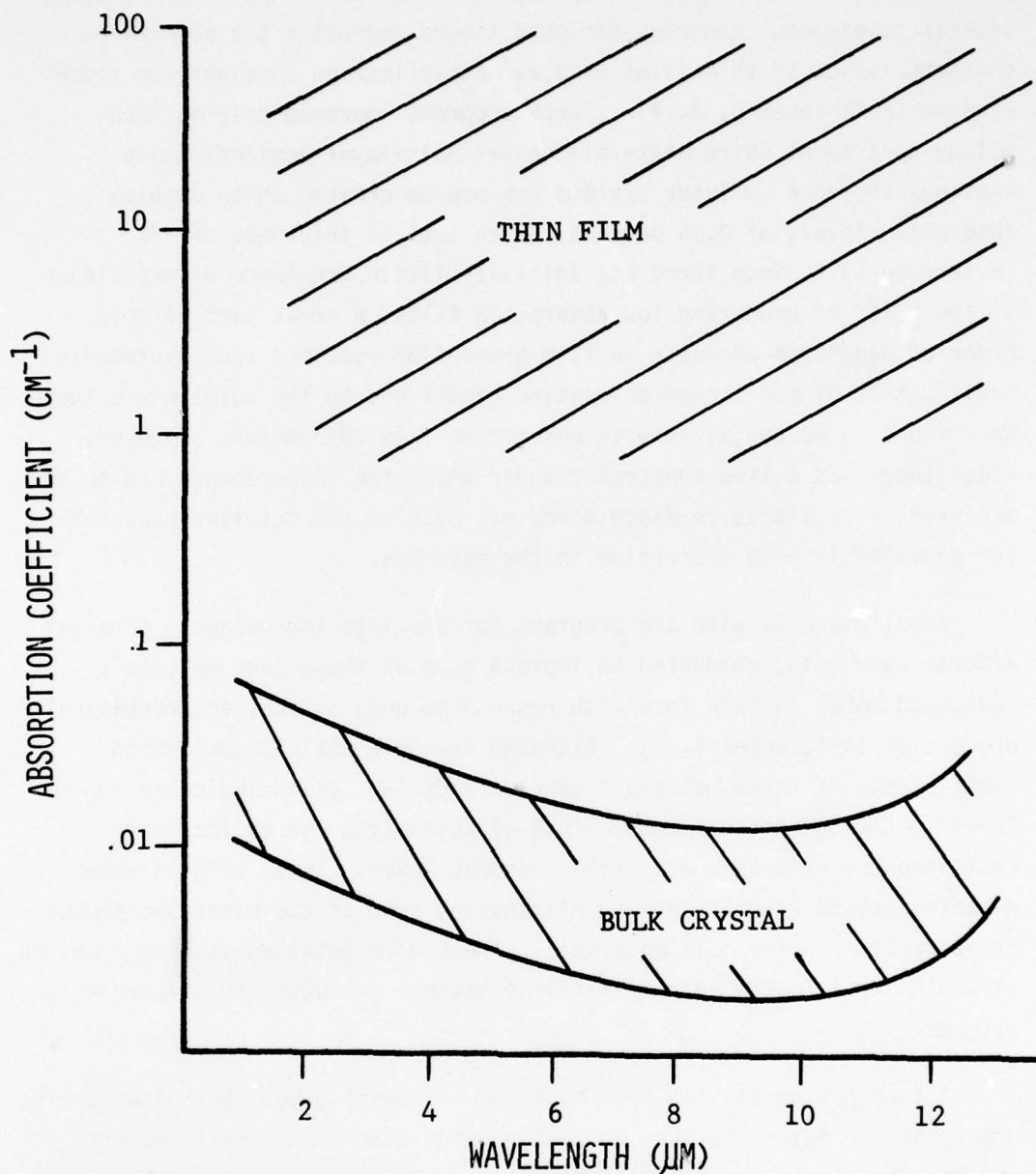


Figure 1. Comparison of Infrared Absorption Coefficients of Bulk ZnSe and ZnSe Thin Films. (Based upon data obtained in this program as well as from Ref. 7,23, 45,48,49,50,51, and 52)

several sources which clearly display the significant differences that have been observed and are still found between the absorption coefficient of ZnSe in the bulk crystalline form and in thin film form.

2. STATEMENT OF THE PROBLEM

Little is known of the exact causes for the anomalously high absorption observed in the coatings used with high power infrared laser systems and, consequently, state-of-the-art absorption levels in thin films are still significantly above bulk values. Therefore, an important need was seen to investigate and identify specific causes for this absorption so that additional techniques might be developed which would result in further decreases in their absorption levels. It was for this purpose that this experimental study was undertaken. Zinc selenide was selected for investigation in this study for primarily two reasons. First, early in the program for the development of window and coating materials for use in high power infrared laser systems, ZnSe was selected as the prime window material and one of two coating materials to be used in a first generation system. This resulted in a significant amount of optical characterization data on ZnSe being made available for baseline use in this study. Second, ZnSe is transparent throughout the wavelength range from 14 μm in the infrared to 0.5 μm well into the visible spectrum; consequently, a large number of analytical techniques peculiar to only selected regions across this transparent range could be used in a complementary manner to describe phenomena observed in the thin film coatings.

3. ORGANIZATION OF THE REPORT

The remainder of this report is divided into four sections. Section II describes previous experimental and theoretical work which provided the framework for the experimental approach taken in this program. Section III describes the experimental program consisting of two subdivisions, the first involving the deposition of the ZnSe thin film coatings under a variety of conditions and the second involving the analysis of these coatings using optical and surface analysis techniques.

Section IV contains a discussion of the results of the experimental program with particular emphasis on their relationship to predictions formulated in Section II. Section V summarizes the conclusions and recommendations resulting from this research program.

SECTION II

PREVIOUS EXPERIMENTAL AND THEORETICAL CONSIDERATIONS

1. GENERAL BACKGROUND

A significant amount of theoretical and experimental work has been devoted to the study and description of absorption processes in semiconductors. Unfortunately, most of this work is concerned only with regions of the optical or infrared spectrum where experimentally measurable quantities of absorbed energy can be used to verify theoretical predictions, for example, close to the band edge, in the long wavelength lattice absorption region, or in regions where impurities produce discrete absorption lines. Noticeably lacking is work relating to absorption in the ultra-low absorption region loosely defined as the frequency range below the fundamental bandgap, but above two to three times the fundamental or transverse optical phonon frequency. With interest in high power laser materials increasing, more emphasis is being directed toward this transparent region as is evidenced by the inclusion of this topic in each of the seven annual conferences on high power infrared laser window materials conducted since 1971 (References 8, 9, 10, 11, 12, 13, 14). Perhaps the most comprehensive single source of information on optical processes in the transparent region is a compilation of both theoretical and experimental topics presented in 1975 at a conference called specifically to discuss this one subject (Reference 15). In this publication, Mitra and Bendow list four mechanisms considered as the main sources of residual absorption in the transparent region: (1) multiphonon processes, (2) various defects and impurities, (3) phonon assisted electronic transitions in the long wavelength tail of the fundamental absorption edge, and (4) multiphoton electronic transitions in the case of high photon flux (Reference 15: vii). Of these four mechanisms all except the second, various defects and impurities, represent intrinsic properties of the semiconductor materials. In a comparison of theoretical absorption and experimental data, Rowe and Harrington have concluded that the absorption coefficient of bulk polycrystalline ZnSe, typically about $3 \times 10^{-3} \text{ cm}^{-1}$ at $10.6 \text{ }\mu\text{m}$, is an extrinsic limit since theoretical predictions indicate an intrinsic limit

in the 10^{-5} cm^{-1} range (Reference 16). Since, as has already been pointed out, the experimentally determined absorption coefficient for ZnSe in thin film form is several orders of magnitude higher than that of ZnSe in bulk form, it is reasonable to assume that extrinsic factors are the primary causes for the high absorption in the thin film coatings. Based upon these factors, the theoretical considerations investigated in this study were limited only to extrinsic absorption mechanisms.

Winsor has categorized extrinsic absorption mechanisms into four groups (Reference 17). Table 2 lists these four categories along with some representative examples of each mechanism. In addition to these, one other source of apparent increase in absorption was investigated by Winsor. This mechanism is initiated by either surface or bulk scattering of radiation which subsequently becomes trapped within the substrate due to total internal reflection. Once trapped, the radiation has a greatly increased probability of being absorbed resulting in a net increase in the overall measured absorption. Using a substrate model based upon a finite coin geometry, Winsor has determined that for substrates having a relatively low refractive index, the increased absorption due to scattering should be negligible (Reference 17). For the case of a substrate with a very high refractive index, the analysis indicates that even in an extreme case, only about a factor of ten times increase in absorption can be expected. Both of the substrates used in the present study, calcium fluoride (CaF_2) and potassium chloride (KCl), have a very low refractive index of about 1.45, and based upon Winsor's scattering model, no significant increase in absorption should be caused by scattering either from within the substrate or by scattering from the ZnSe coating on the substrate. Consequently, no direct investigation of absorption induced by scattering was made in this study.

Pursuing the assumption that the anomalous absorption in the transparent region of ZnSe coatings is due to one or more of the extrinsic mechanisms listed in Table 2, each mechanism was considered separately and a preliminary ordering of the categories was made based upon the probable relative importance of each. Listed lowest in order of importance was electronic defects. This was primarily due to the fact

TABLE 2
EXTRINSIC ABSORPTION MECHANISMS

<u>Microscopic Lattice Defects</u>	<u>Macroscopic Lattice Defects</u>	<u>Electronic Defects</u>	<u>Surface Defects</u>
Interstitial	Grain Boundary	Traps	Adsorbed Impurities
Vacancy	Inclusion	Excitons	Coating/Substrate Interaction
Impurity		Color Centers	Surface Condition

that this absorption mechanism would most likely produce some degree of structure in the absorption spectrum. However, absorption measurements made on thin films at several wavelengths in the infrared spectrum indicated that the absorption occurs as an overall increase across the spectrum rather than at unique wavelengths. Placed next in order of importance was the category of surface defects. Although there were no significant a priori reasons to assume that surface and interface effects contribute less to absorption than do the effects included in the remaining two categories, early experimental results from this study led to this conclusion. These results will be discussed in a later section. The remaining two categories could not be separated by degree of contribution to absorption and, therefore, were considered as a single category which encompassed all lattice defects.

2. RELATED EXPERIMENTAL WORK

As is indicated by Table 2, there are several examples of macroscopic or microscopic lattice defects, any of which could cause an increase in absorption over that of an otherwise perfect crystal. Although, as has been mentioned before, there has been little work done in the past relating these mechanisms to absorption in transparent films, there have been investigations into the effects that various defects have on the electrical characteristics of these films. With respect to ZnSe and other compounds composed of elements from Group II and Group VI of the periodic chart, some significant studies of electrical properties of films have been made which can be applied to the problem of absorption. Additionally, infrared absorption studies made of some of these same materials in bulk form have also pointed out possible causes for the increased absorption observed in ZnSe films. Both the bulk crystalline and thin film studies have centered around the measurable changes which occur under different deposition or growth conditions. In a significant number of these investigations, results have tended to infer that changing growth conditions can affect the stoichiometry of the material and consequently the electrical and optical properties. These stoichiometric variations have been observed in several different

forms in which either an excess or a deficiency of one of the elements existed as a vacancy, an interstitial, or as an inclusion (References 18, 19, 20).

Some results of investigations of thin films of II-VI materials include those of Snedjar et al. who reported that thermally evaporated CdSe films show a predominance of Se vacancies and a resultant low resistivity (Reference 19). Subsequent annealing in Se vapor increased the resistivity to that of bulk CdSe. Similarly, Moore et al. report that CdSe films exhibit an excess of Cd which can be inhibited by carrying out the deposition at high substrate temperatures while providing excess Se in the vapor stream (Reference 20). Foster has found that direct evaporation of CdS yields films having low resistivities caused by sulfur vacancies, but coevaporation of CdS and S produces high resistivity films (Reference 22). In their studies on CdTe thin films, Glang et al. found that films deposited at low substrate temperatures showed a lower transmission in the 0.8 to 1.5 μm range than those deposited at higher temperatures (Reference 20). This was attributed to the presence of free tellurium in the higher absorbing film. Finally, Rood noted that ZnS films deposited at high deposition rates exhibited considerably higher optical absorption than those deposited at low rates (Reference 18).

Although there is a noticeable deficiency of similar data relating to the properties of ZnSe thin films, this is not the case for ZnSe in bulk crystalline form. The effect of crystal growth conditions on the infrared absorption in polycrystalline ZnSe has been investigated for growth techniques including chemical vapor deposition (CVD), physical vapor deposition (PVD), as well as growth from the constituent elements. The CVD process has produced the lowest absorbing bulk ZnSe to date and involves the reaction of H_2Se with Zn vapor in a temperature controlled furnace and the subsequent condensation of the solid ZnSe onto a suitable surface. Growth studies have shown that the lowest absorbing ZnSe produced by the CVD method is obtained with H_2Se to Zn molar ratios greater than 1.0 and that a deposition temperature of 700°C is inferior to one of 750°C (Reference 7). Similarly for the case involving growth

by reacting elemental Zn and Se, it was found that a Se to Zn molar ratio of 1.25 to 1.64 resulted in the lowest absorbing ZnSe material (Reference 23). However, for the PVD case in which solid ZnSe is heated until it dissociates into Zn and Se_2 and then is allowed to condense onto an appropriate surface, there is no control of the Se to Zn molar ratio which is presumably very close to a value of 1.0. This PVD method is essentially the same technique involved in the deposition of thin films using the thermal or electron beam evaporation techniques. Bulk ZnSe which has been grown by the PVD method has been found to have significantly higher infrared absorption than that observed in material grown by either of the other two methods (Reference 23). Shiozawa et al. have investigated the infrared absorption of both bulk ZnSe and bulk CdTe grown by the PVD method. In their studies on ZnSe they found that the as-grown material contained Se vacancies but that subsequent annealing of the ZnSe in Se vapor aided in decreasing the number of these vacancies while simultaneously producing a significant reduction in the infrared absorption (Reference 6). Table 3 summarizes the $10.6 \mu\text{m}$ absorption coefficients that have been measured for ZnSe grown by each of the three methods. This comparison clearly indicates the advantage that control of the Se to Zn molar ratio offers in the CVD and elemental growth techniques. Also included in this table are the effects that post growth treatments have produced in PVD grown ZnSe.

TABLE 3
ZnSe ABSORPTION COEFFICIENT

<u>Growth Method</u>	<u>Absorption Coefficient (cm^{-1})</u>	<u>Reference</u>
CVD	0.001	7
Elemental	0.002	22
PVD	0.012-0.05	22
PVD	1.0 Prior to Anneal; 0.2 After Anneal	6

In the investigation of PVD grown CdTe, Shiozawa noted similar results to those found with the PVD grown ZnSe; however, in this case vacancies involving the Group II component (Cd) were observed rather than those of the Group VI component (Te). As was expected, post growth annealing in Cd vapor brought about a noticeable reduction in the infrared absorption (Reference 6). The fact that CdTe was found to have a deficiency of Cd rather than Te can be explained with the aid of Figure 2 which shows the vapor pressure curves for each of the five elements normally considered to form the II-VI semiconductor compounds. For all II-VI compounds except those containing Te, the Group II element is seen to have a lower vapor pressure than the Group VI element; for compounds containing Te, the opposite is true. In the studies made on both thin films and on PVD grown crystals it was always observed that the stoichiometry of the compounds tended to show a deficiency of the more volatile component.

3. THEORETICAL CONSIDERATIONS

Gunther has proposed a theory describing the condensation of thin films of binary compounds in which he shows that particularly for compounds whose constituent elements have significantly different vapor pressures, large deviations in the stoichiometry of the deposited films can be expected (Reference 25: 213-232). An understanding of this theory and its particular application to the growth of ZnSe films is best achieved by first reviewing some aspects of the processes involved in the nucleation and growth of single component films.

When an incident flux, N_+ , of vapor atoms impinges on a surface, initially two conditions can occur. First the atom can be immediately reflected back into the vapor stream or second, the atom can be absorbed onto the surface. In the absorbed state the atom possesses a surface mobility which allows it to diffuse somewhat freely along the surface. If, during the process of diffusion, the atom arrives at a nucleation or growth site, condensation takes place whereby the atom becomes tightly bound to the surface. However, prior to arriving at a nucleation site it

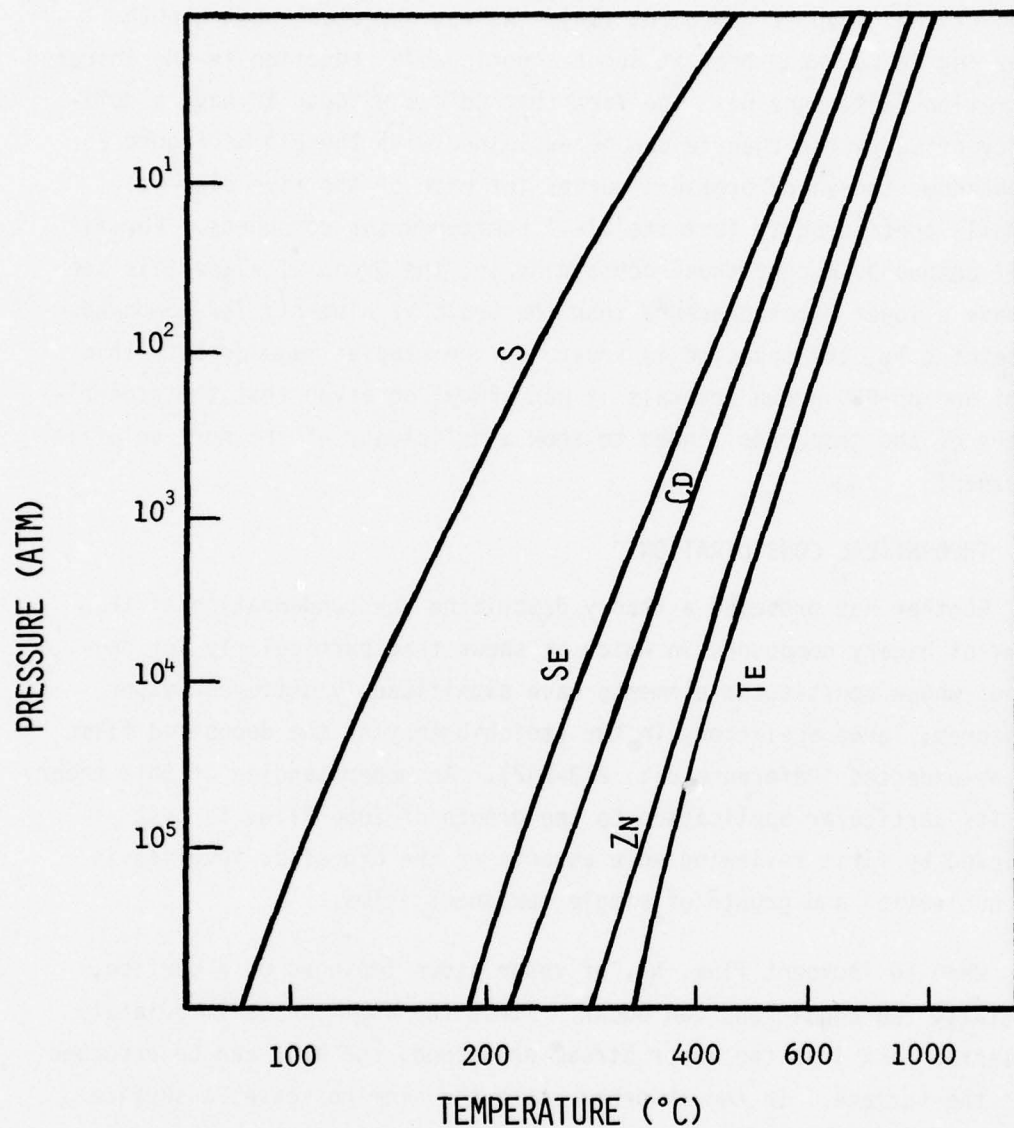


Figure 2. Vapor Pressures of Elements Comprising the II-VI Compounds. (From Ref. 53)

is still possible for the atom to free itself from the surface and be reemitted back into the vapor stream. The net rate of condensation, N_k , is then defined as

$$N_k = N_+ - N_e \quad (2)$$

where N_+ is the incident flux, and N_e is the sum of the reflected and reemitted flux. It is well known that N_k is intimately related to both the substrate temperature T_s and the incident flux N_+ and in particular for a constant N_+ there is a critical substrate temperature T_{c_+} above which N_k becomes zero, that is no film growth will occur. Similarly, for a constant T_s there is a critical incident flux N_{+c} below which N_k becomes zero.

Gunther has used these concepts of single component film growth to develop his theoretical description of the growth of a binary compound formed from separate constituents A and B both of which have a vapor pressure which is greater than that of the compound AB. This theory reasonably assumes that the vapor densities of the constituents in the impinging stream are low enough so that collisions within this vapor stream can be neglected. However, once the atoms have entered the adsorbed phase, it is required that an interaction of the constituents occur which results in the formation of the compound AB. Figures 3 and 4 are graphical representations which have been derived from Gunther's description of the deposition process. In these figures are shown the changes in film composition which are brought about by different growth conditions. In the particular case shown, component B is depicted as having a higher vapor pressure than that of component A. Referring to Figure 3, the incident flux of component A and component B are plotted on the ordinate and abscissa respectively. For a constant substrate temperature T_1 , the critical flux values for the single component deposition of components A and B are also depicted and represented by the lines labeled N_{c_A} and N_{c_B} . If one starts with the condition of very low values for N_{+A} , then it is seen that for all values of N_{+B} which are below N_{c_B} , no condensation of any kind will occur. However, for a

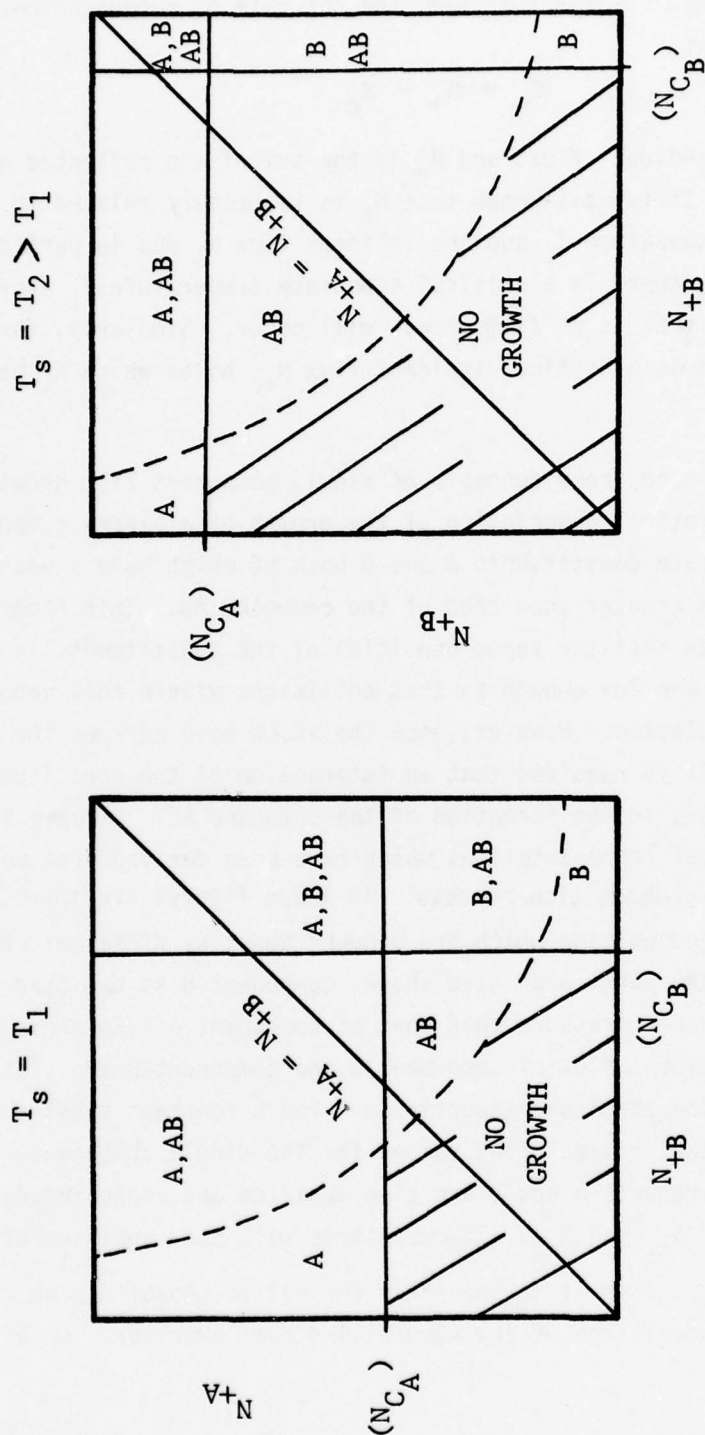


Figure 3. Variation of Film Composition with Incident Flux

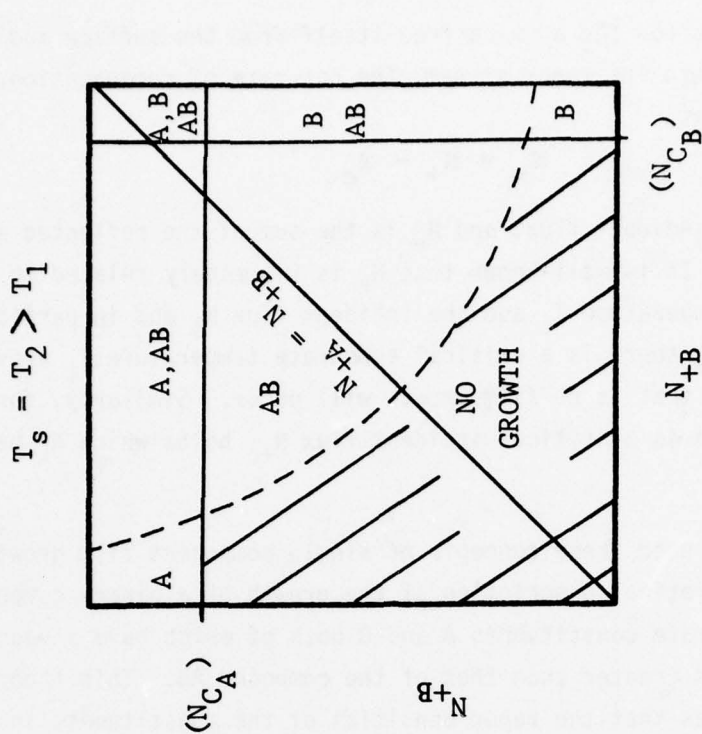


Figure 4. Variation of Film Composition with Incident Flux at Elevated Temperature

constant value of N_{+B} , as N_{+A} is allowed to increase, a condition is eventually reached when the deposition of the component AB is initiated. The value of N_{+A} for which this stoichiometric deposition is found to occur depends upon the selected value of N_{+B} but is seen to be lower than N_{C_A} . As N_{+A} is increased beyond N_{C_A} , the A constituent as well as the compound AB begins to condense simultaneously and the film composition shifts from being stoichiometric to having an excess of component A. Figure 4 shows the effects on this process which are caused by increasing the substrate temperature to a value T_2 which is greater than T_1 . As is the case with single component evaporation, this causes the critical values, N_{C_A} and N_{C_B} , to be increased and broadens the range of values of N_{+A} and N_{+B} in which a stoichiometric film can be attained.

For the particular case of equal flux values, $N_{+A} = N_{+B}$, this theoretical description predicts that very high flux rates result in highly nonstoichiometric films. However, as the flux rates are lowered, the film tends to become more stoichiometric. Also, under these equal flux conditions, it is seen that a high substrate temperature again provides a greater probability for obtaining a stoichiometric film.

Gunther has experimentally verified this theory by conducting deposition studies with CdSe using what has become known as the three-temperature method of deposition (Reference 25: 213-232). In this study, he evaporated elemental Cd and Se from separate furnaces and controlled the incident flux of each by separately varying the individual furnace temperatures. A third control was obtained by being able to vary the substrate temperature. The results of these experiments are summarized in Figure 5. The Cd flux was maintained at a constant level of about $2 \times 10^{16}/\text{cm}^2/\text{sec}$ and the Se flux was varied from 10^{15} to $10^{18}/\text{cm}^2/\text{sec}$. Stoichiometric variations of the thin films were measured by means of Debye-Scherrer x-ray analysis. At a substrate temperature of 200°C , low selenium flux values resulted in no condensation; however, at higher flux levels a broad region of stoichiometric condensation was achieved. Once the very high Se flux rates were attained, the results indicated the films contained large excesses of Se. When the experiment was repeated at a

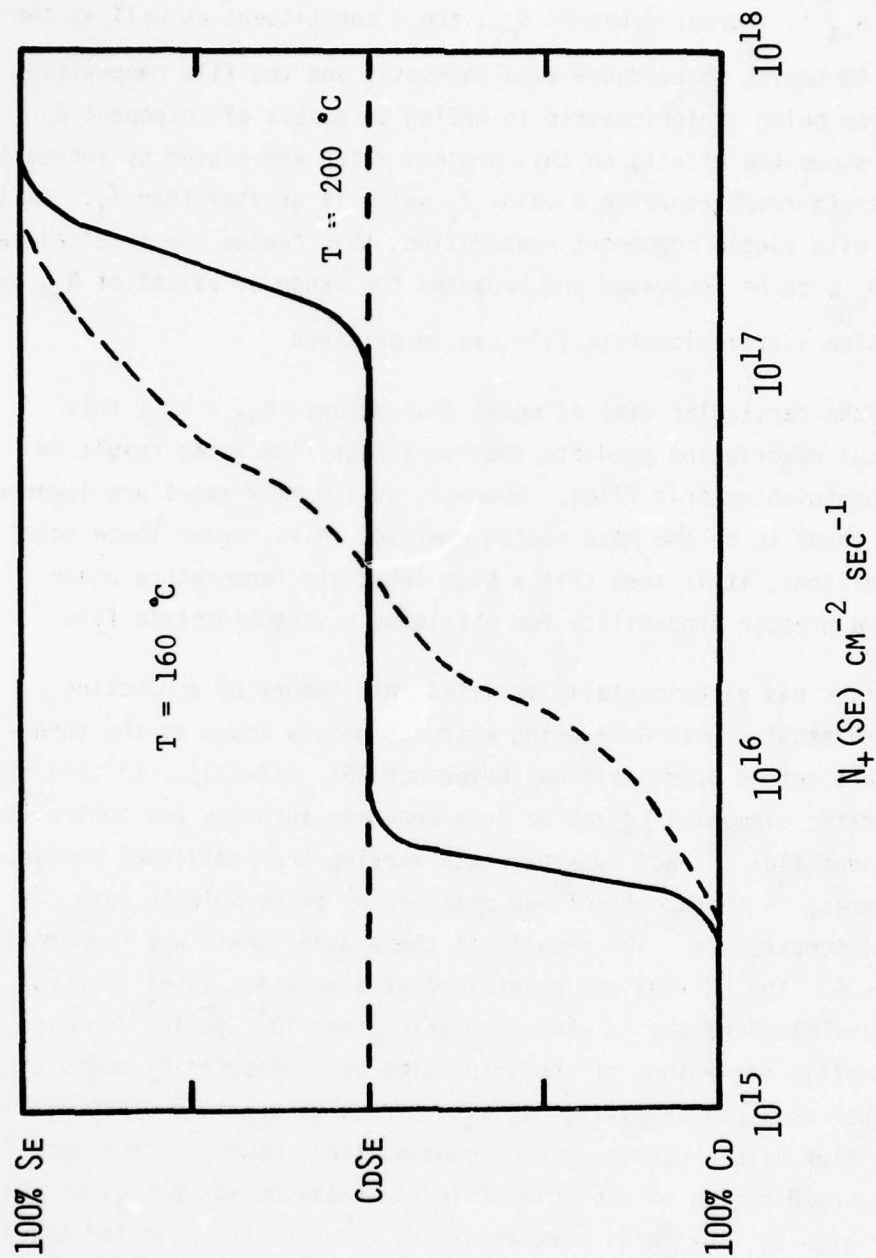


Figure 5. Composition of Condensed CdSe Layers as a Function of Incident flux. ($N_+(\text{Cd}) = 2 \times 10^{16}\text{ cm}^{-2}\text{ sec}^{-1}$) (From Ref. 25)

lower substrate temperature (160°C), a different behavior was observed. Unlike the case for the high substrate temperature in which a stoichiometric composition resulted for a wide range of incident flux values, at the lower temperature it proved to be difficult to produce a stoichiometric film for almost all values of incident flux. Rather, as the Se flux was increased, a gradual change from Cd rich to Se rich composition was observed. All of these results were in agreement with the theoretical behavior predicted by Gunther.

Evaluating the results of past experiments with II-VI compounds in light of the deposition theory of Gunther, there appears to be strong evidence to conclude that a significant part of the anomalously high absorption found in ZnSe thin films could be due to a nonstoichiometric deposition of the coating. In particular, the Zn and Se vapor pressure curves would cause one to conclude that these films would tend to be rich in Zn. The nature of this excess Zn in ZnSe is not clearly defined, but it can reasonably be classified as a microscopic or macroscopic lattice defect as described earlier; that is, it could possibly occur as condensed Zn metal inclusions or as Zn interstitials in the ZnSe lattice. Conversely, the apparent excess Zn could in actuality be the result of a deficiency of Se in the form of Se vacancies. This latter defect has been observed in several other nonstoichiometric II-VI compounds. In these cases it was felt most likely that the Se vacancies precipitated out, resulting in localized voids in Zn-rich areas.

The effect that such defects have on the infrared absorption in a material has not been defined. However, two theoretical approaches have been examined to obtain an "order-of-magnitude" estimate of the absorption increases that might be observed in such cases. Both approaches use models based upon the existence of small absorbing particles in a non-absorbing host matrix where the particle dimensions are much less than those of the wavelength of the absorbed radiation. The first approach is that of Sparks who looked at absorption cross section calculations based upon limiting cases of Mie Theory (Reference 26). The absorption coefficient (β) can be expressed as

$$\beta = \sigma_{abs} N_I \quad (3)$$

where N_I is the number of inclusions per unit volume and σ_{abs} is the absorption cross section which itself is a function of the wavenumber (k), the particle radius (a), and the particle complex dielectric constant (ϵ). Employing a model based upon the inclusions being small metallic spheres, Sparks assumed a Drude approximation to the dielectric constant of the form

$$\epsilon = \epsilon_{\infty} - \frac{\omega_p^2}{\epsilon_H(\omega^2 + i\omega\Gamma)} \quad (4)$$

Here, ϵ_{∞} is the contribution to ϵ from the core electronics, ω_p is the plasma frequency, and ϵ_H is the dielectric constant of the host material. Γ is the electron relaxation frequency which Sparks indicates for inclusions having dimensions less than 200 Å can be approximated as V_f/a with V_f being the Fermi velocity, typically about 10^8 cm/sec for metals. With the further assumption that

$$\omega_p^2 \gg |\omega^2 + i\omega\Gamma| \quad (5)$$

the absorption cross section can be expressed as

$$\sigma_{abs} \approx 12 \epsilon_H^{3/2} \frac{\omega^2}{\omega_p^2} \frac{\Gamma a}{c} \pi a^2 \quad (6)$$

Additionally, introducing the refractive index (n) defined by the relation

$$n = \sqrt{\epsilon} \quad (7)$$

the final expression for the absorption coefficient takes the form

$$\beta = \frac{9n_H^3 \omega^2 \Gamma}{c \omega_p^2} f \quad (8)$$

where the volume fraction ($f = 4/3 \pi N_I a^3$) represents the total volume of absorbing inclusions per unit volume of host material.

Bowen and Vander Sande have also attempted to calculate the magnitude of the absorption cross section for the purpose of estimating the amount of absorption which can be expected in a non-absorbing material

containing absorbing particles (Reference 23). They similarly assumed the expression for the absorption coefficient to be

$$\beta = \sigma_{\text{abs}} N_I \quad (3)$$

but, based their calculations of the absorption cross section on Rayleigh scattering by particles having a finite conductivity. They assumed that the cross section was related to the particle polarizability (γ) by the expression

$$\sigma_{\text{abs}} = \frac{4\pi}{k^2} \operatorname{Re}[i k^3 \gamma] = -4\pi k \operatorname{Im}(\gamma) \quad (9)$$

where k again is the wave number equal to $2\pi/\lambda$.

Since the particles are defined to be small compared to the radiation wavelength, they are assumed to exist in a uniform electric field. This allows the polarizability to be determined through the familiar Clausius-Mosotti equation to yield the expression

$$\gamma = \frac{\hat{n}_p^2 - 1}{\hat{n}_p^2 + 2} a^3 \quad (10)$$

with (a) being the particle radius and \hat{n}_p the complex refractive index of the particle. Using this expression for the polarizability and taking into account the refractive index of the host material (n_H), Equation 3 becomes

$$\beta = \frac{-8\pi^2 n_H}{\lambda} \operatorname{Im} \left[\frac{\left[\frac{\hat{n}_p}{n_H} \right]^2 - 1}{\left[\frac{\hat{n}_p}{n_H} \right]^2 + 2} \right] f \quad (11)$$

Equation 8 and Equation 11 have been used to construct the curves shown in Figure 6 which give an estimate of the volume fraction of excess Zn necessary to cause the high values of the absorption coefficient observed in ZnSe thin films. For the curves relating to Spark's theory, a particle size dependency is seen to exist which enters through the relaxation frequency (Γ). Only a single curve is shown for the Bowen

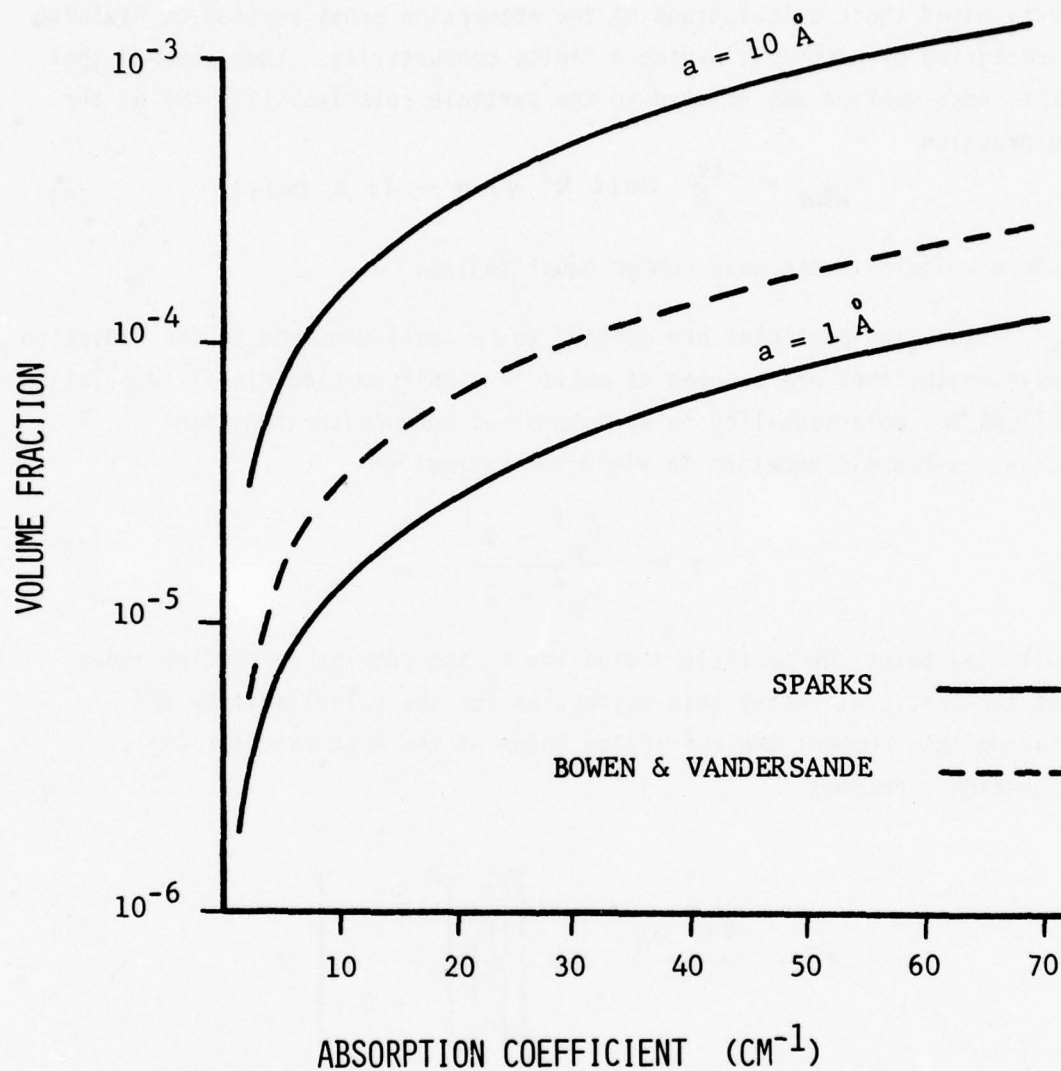


Figure 6. Theoretical Excess Volume Fraction of Zn Required to Produce Observed $1.06 \mu\text{m}$ Absorption in ZnSe.

and Vander Sande model since no particle size dependency exists for this case. Table 4 lists the values assigned to the constants which were used in Equations 8 and 11 to arrive at Figure 6. It should be noted that these calculations are based on a radiation wavelength of 1.06 μm . This was the wavelength at which absorption measurements were conducted in the experimental portion of this program. The reason for selecting this wavelength will be explained later in the Experimental Section.

Figure 7 shows the results obtained from Equations 8 and 11 expressed in a somewhat different manner. Here, the volume fraction has been replaced by the particle number density to give an indication of the size of the particles that would be required at a fixed concentration level to cause an increased absorption level to be measured. Again the "order-of-magnitude" estimate shows that nominally small particles ($< 100 \text{ \AA}$) at reasonable concentration levels ($10^{15} - 10^{18}/\text{cm}^3$) are capable of causing significant increases in the measured absorption coefficient.

TABLE 4
PARAMETERS USED TO CALCULATE ABSORPTION COEFFICIENT

<u>Parameter</u>	<u>Symbol</u>	<u>Value</u>	<u>Reference</u>
Wavelength	λ	1.06 μm	--
Refractive Index (Zn)	\hat{n}_p	2.53-i 2.37	27
Refractive Index (ZnSe)	n_H	2.48	28
Radiation Frequency	ω	$1.8 \times 10^{15} \text{ Hz}$	--
Plasma Frequency (Zn)	ω_p	$1.45 \times 10^{16} \text{ Hz}$	29
Relaxation Frequency	Γ	$10^8/a \text{ sec}^{-1}$	26

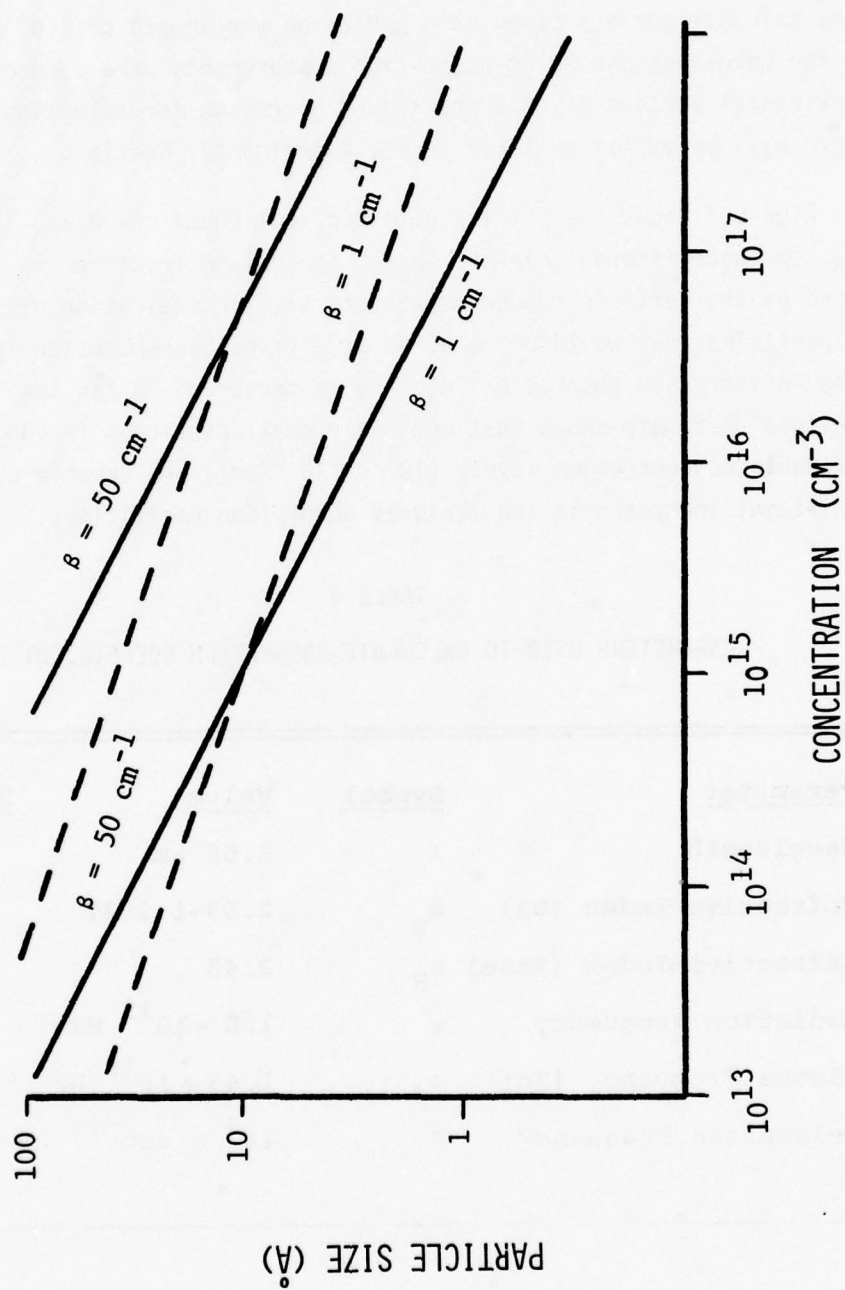


Figure 7. Theoretical Relationship Between Zn Particle Size and Concentration Required to Produce Increased 1.06 μm Absorption in ZnSe.

SECTION III

EXPERIMENT

1. OVERVIEW

The experimental portion of this project was designed to investigate whether or not the optical characteristics and particularly the infrared absorption of ZnSe thin films could be changed significantly by varying the deposition conditions. Further, if this were found to be true, would the changes be consistent with theoretical predictions based upon changes in stoichiometry? If a stoichiometric variation was one of the significant factors in causing increased absorption in thin films then the following trends would be expected:

1. High substrate temperatures would be conducive to improved stoichiometry and lower absorption.
2. Lower deposition rates would be conducive to improved stoichiometry and result in lower absorption.
3. Excess Se in the vapor stream would provide a means for improving stoichiometry and lowering absorption.

The experimental procedure used in this study is outlined in Figure 8. Substrates to be coated were first optically polished and cleaned. The uncoated substrates were then evaluated using laser calorimetry to determine the baseline absorption level in each. Four of the substrates were next placed in a vacuum chamber and coated with a thin film of ZnSe using electron beam evaporation. All four substrates were coated under identical conditions except for the fact that a different film thickness was deposited on each. After being coated, the substrates were again evaluated by laser calorimetry in order to determine the increase in absorption produced by the thin film of ZnSe. Subsequent to this, additional analytical measurements were performed on these samples which included spectrophotometric transmission and ellipsometry measurements to determine the refractive index of the films. Nomarski interference microscopy was used to qualitatively characterize the surface of the film-substrate combination and to reveal

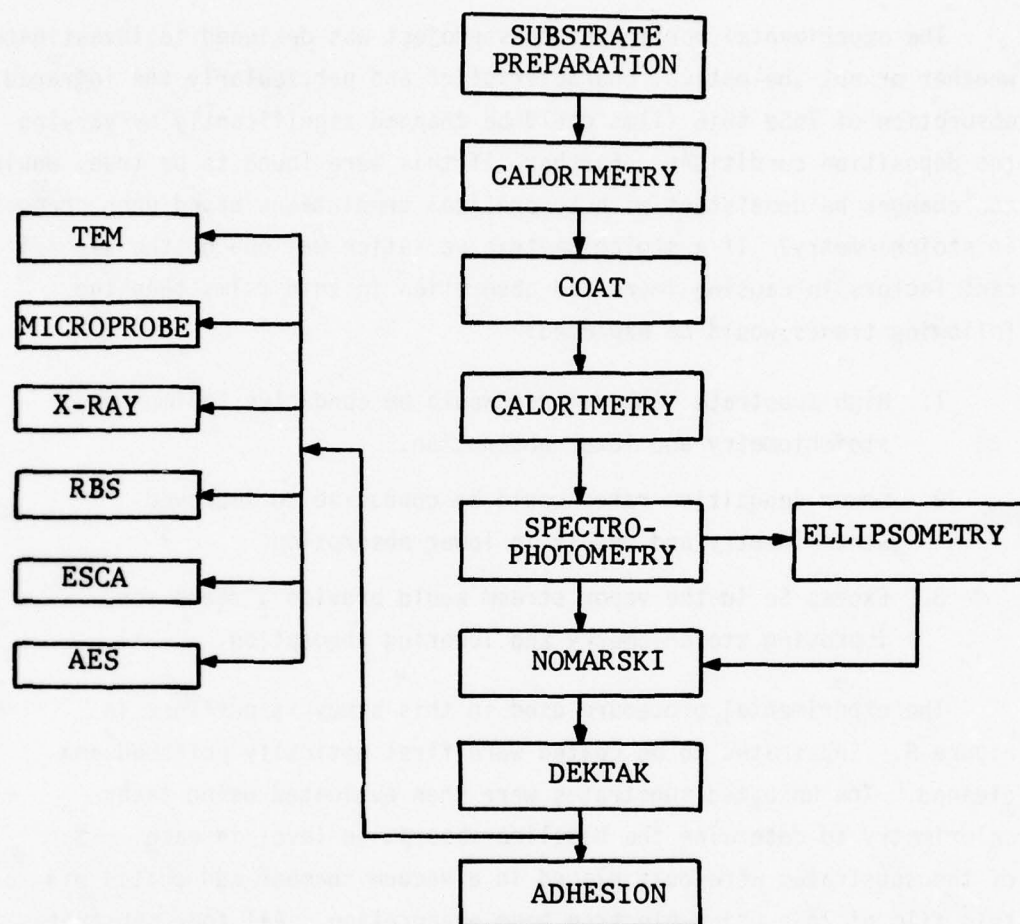


Figure 8. Flow Chart of Sample Preparation, Coating, and Evaluation

if different surface conditions resulting from substrate polishing were producing any measurable effect on absorption. Film thickness was next determined using a Dektak surface profile measuring system. Finally a qualitative measure of film adhesion was made using pressure sensitive tape and water immersion. The films were then removed from the substrates which were subsequently repolished in preparation for being coated again with ZnSe under a different set of deposition conditions. In several cases, coated substrates or companion witness plates were selected for additional analysis by one of several surface analysis or characterization techniques. These techniques were employed primarily in an attempt either to directly determine film stoichiometry or to detect the presence of impurities in these films. The remainder of this section contains a more detailed discussion of the materials, equipment, procedures, and analytical techniques used in this study.

2. SUBSTRATES

For CO₂ laser systems operating at a wavelength of 10.6 μm , potassium chloride (KCl) is the material which has been emphasized most for use as a laser window. The reason for this is that it is one of the very few materials which has reasonable strength and which is non-absorbing at 10.6 μm . The absorption coefficient at this wavelength is about $5 \times 10^{-4} \text{ cm}^{-1}$. For these reasons, KCl was initially selected as the substrate material for use in this program. However, it was quickly determined that the detrimental properties of KCl made it unsuitable for use in a study of this kind. KCl has two serious drawbacks. First, polishing of the soft surface is extremely difficult and, in fact, methods are still being studied to perfect this capability (References 30, 31). Because KCl is hygroscopic, extreme care must be used both in handling the substrates and in insuring that a high humidity environment is not allowed to produce damaging effects on the surface. Early attempts at measuring absorption in coated KCl during this program resulted in inconsistent data. This was attributed to increased substrate absorption brought on by changing surface conditions. These changing surface conditions

made the determination of a baseline absorption level impossible and, consequently, an alternate substrate material had to be selected.

Low substrate absorption was the overriding concern in selection of a new material since detection of the slight increase in absorption in the very thin coating of ZnSe depended on the substrate having the lowest possible baseline absorption level. Calcium fluoride (CaF_2) was found to possess the desired properties, but only at wavelengths shorter than 9 μm . At longer wavelengths it no longer remains transparent. Selection of CaF_2 precluded the measurement of absorption at 10.6 μm but the possibility of using a 5.3 μm carbon monoxide laser or a 1.06 μm Nd:YAG laser for calorimetric absorption measurements presented a viable alternative. The latter wavelength was finally selected primarily because of the availability of equipment. Early absorption measurements also revealed an additional benefit in the choice of the 1.06 μm system. It was found that the CaF_2 substrate absorption decreased significantly upon going to the shorter wavelength; however, the ZnSe coating absorption remained at a somewhat constant level that seemed to be independent of wavelength. This, in effect, resulted in an increase in the sensitivity of the calorimetric measurement.

The substrates used for the coating experiments were 5 cm diameter by 1 cm thick polycrystalline CaF_2 made by Harshaw Inc. The substrates were initially received with an "inspection shine" surface finish but were subsequently polished prior to being coated with ZnSe. The following procedure was used in polishing the CaF_2 :

1. Polish on an 8 in. bronze wheel covered with silk (Buehler) at 550 rpm while applying medium pressure and using a 1.0 μm $\text{Al}_2\text{O}_3/\text{H}_2\text{O}$ slurry.
2. Repeat step 1 using 0.3 μm Al_2O_3 .
3. Polish on an 8 in. wheel covered with Buehler Microcloth using medium pressure and a slurry of 0.05 μm $\text{Al}_2\text{O}_3/\text{H}_2\text{O}$.

Prior to determining a baseline absorption level for the uncoated substrates, each substrate was also cleaned using the following procedure:

1. Rinse in distilled water.
2. Submerge in standard Alconox solution and gently wipe the surfaces.
3. Rinse in flowing distilled water.
4. Rinse in flowing isopropyl alcohol.
5. Blow dry in a gently flowing air stream.
6. Repeat steps 1 through 5.

A total of twelve separate CaF_2 substrates were used during the course of this study with four of these being coated during each coating run. Once all measurements had been completed on the set of four coated substrates, each substrate was repolished and cleaned using the above described procedures in preparation for additional coating runs.

3. COATING DEPOSITIONS

A preliminary experimental investigation of ZnSe coating techniques which included flash evaporation, thermal evaporation, and electron beam evaporation was carried out and resulted in the selection of electron beam evaporation as the best method for depositing the coatings to be studied. This choice was based on the fact that electron beam evaporation provides excellent control of evaporation rate and eliminates variations in substrate temperature caused by thermal radiation inherent in the other two methods. Additionally, electron beam evaporation minimizes the possibility of evaporated impurities condensing in the films since only the evaporation source material itself is heated. The source material for all depositions was Raytheon CVD ZnSe.

The electron gun source used was a Varian Model 980-0003 rated at 2 kw. This was a three crucible water cooled system which could be mechanically moved along one direction. All evaporations were made

from the center crucible; the linear motion capability was used to reposition the electron beam as the source material evaporated. The high voltage for this system was obtained from a Universal Voltronics 4 kV high voltage power supply, Model 4-450. This supply possesses a variable high voltage capability which allowed additional electron beam positioning along a direction perpendicular to that provided by the mechanical motion of the crucible. Thus, an independent X-Y beam positioning capability existed which permitted beam placement anywhere on the surface of the source material. Power for the electron emission source was provided by a Varian Associates e-Gun Control Unit, Model 922-0020 which was modified to allow the use of the separate high voltage power supply. The deposition rate was controlled by means of a Sloan Instruments Corporation Automatic Deposit Control Unit, Model OMNI. This unit is a combination of a Sloan Deposit Rate Control, Model DRC and a Sloan Deposit Thickness Monitor, Model DTM-2A. The DTM-2A is a quartz crystal film thickness monitor which provides an electrical output signal to the DRC, the derivative of which is proportional to the film deposition rate. The DRC in turn provides a feedback signal to the emission power supply which allows maintenance of the deposition rate at a constant, preset level.

During a coating run, the four substrates and one glass witness plate were supported on a circular aluminum plate mounted 34 cm above the source material. The center of each substrate was positioned over a separate opening on the circular plate at a point 9.5 cm from its center. In this manner each substrate was equidistant from the evaporation source. In addition to this, each substrate was tilted back so that the vapor stream was incident normal to its surface. A rotatable shutter was placed below the plate and when initially opened all substrates were exposed to the ZnSe vapor stream. Then, at predetermined intervals, the shutter was closed in a step-wise manner with an additional substrate being blocked from the vapor stream at each step. In this manner, coatings of different thicknesses could be deposited under identical deposition conditions. A substrate heater was used which consisted of a single reflector enclosing five 420 watt quartz lamps (General Electric-FAL). The lamps were connected in parallel with each

lamp situated 9 cm above one of the substrate positions. A rheostat was used to control the lamp voltage and heat output. The substrate temperature was determined by monitoring the temperature of a 2.5 cm diameter by 1 cm thick piece of KCl placed beside one of the CaF_2 substrates. Two iron-constantan thermocouples were imbedded in the KCl, one near its surface and the other in the center of the material. Both thermocouples indicated the same temperature once a steady-state condition was achieved. This method was calibrated against similar measurements using a bulk piece of CaF_2 as well as with surface temperature measurements made by placing thermocouples directly in contact with the CaF_2 substrates. At a substrate temperature of 75°C all measurements agreed to within 10 percent.

The entire deposition system was contained in an 18 in. diameter bell jar which was pumped by a 6 in. water cooled oil diffusion pump (Consolidated Vacuum Corp. Type-PMC, Model 6B) and a Welch Model 1397 mechanical pump. With liquid nitrogen trapping a vacuum of better than 1×10^{-6} torr could be achieved with this system. A view of the interior of the vacuum chamber showing the components described above is contained in Figure 9.

4. ANALYTICAL MEASUREMENTS

Absorption. As stated previously, a variety of analytical measurements were made on the coated substrates with primary emphasis being placed upon the determination of film absorption by laser calorimetry. Calorimetry is a very sensitive technique for measuring small absorption coefficients of transparent materials and is most applicable in cases where determination of a small energy loss by measuring the difference between input and output beam intensity is impractical because of the difficulties involved in subtracting two large numbers to obtain an extremely small number. To overcome this difficulty, the laser calorimetry technique indicates the amount of absorption occurring within a material from measurements of the temperature rise caused by the absorption of laser radiation as the beam passes through it. The actual power absorbed in the material is determined from the relation

$$P_{\text{abs}} = mC_p \frac{\Delta T}{\Delta t} \quad (12)$$

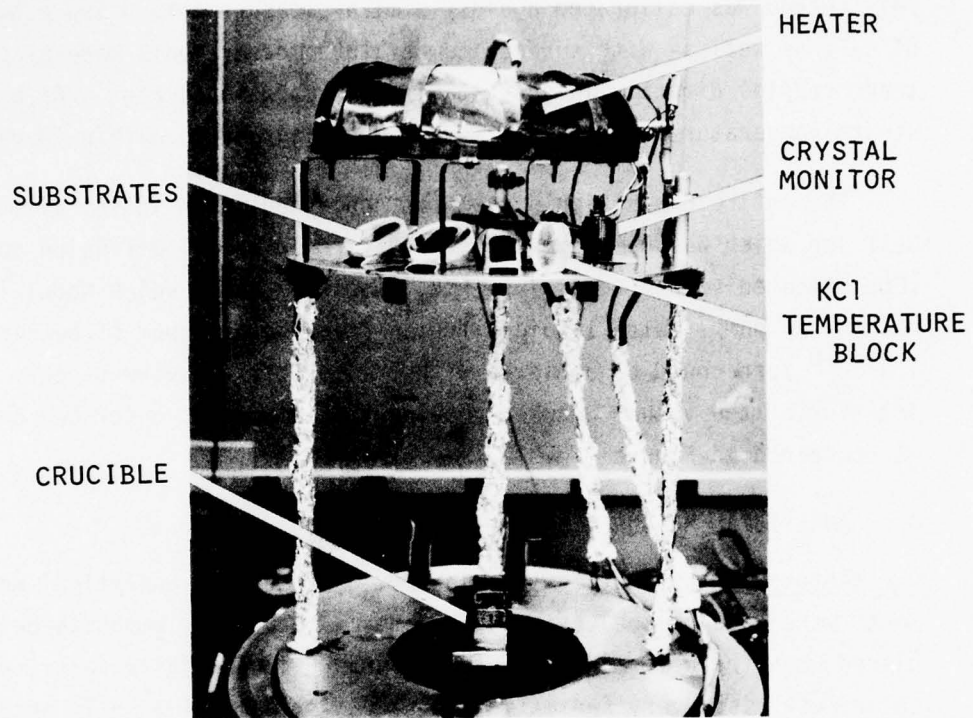


Figure 9. Interior View of Vacuum Chamber

where m is the mass of the sample, C_p is the specific heat of the sample, and ΔT is the increase in temperature observed during the time interval Δt . The power lost from a beam as it passes through a sample can also be obtained from the Beer-Lambert Law

$$P(x) = P_0 e^{-\beta x} \quad (1)$$

where $P(x)$ is the beam power at a position x cm from the entrance face. For small βx , a linear approximation for $e^{-\beta x}$ may be used resulting in an expression for the absorption coefficient of the form

$$\beta = \frac{P_{abs}}{P_0} x \quad (13)$$

By knowing the reflection and transmission coefficients at the exit surface of the material which can be obtained from the refractive index, and by taking into consideration multiple internal reflections, either coherent or incoherent, Weil has shown (Reference 32) that the absorption coefficient expressed in Equation 13 can be rewritten in the form shown below.

$$\beta = \frac{1}{L} \frac{P_{abs}}{P_T} \frac{2n}{n^2 + 1} \quad (14)$$

where L is the sample thickness, n is the refractive index, and P_T is the power transmitted out of the sample. Combining Equation 12 and Equation 14 results in an expression containing all the measurable parameters required to determine the absorption coefficient of a slightly absorbing material:

$$\beta = \frac{mC_p}{LP_T} \frac{\Delta T}{\Delta t} \frac{2n}{n^2 + 1} \quad (15)$$

The calorimeter used to determine absorption coefficients in this study is represented schematically in Figure 10. The 50 mm diameter sample to be measured was supported and thermally isolated by three equally spaced nylon pins held in place by an aluminum ring having an

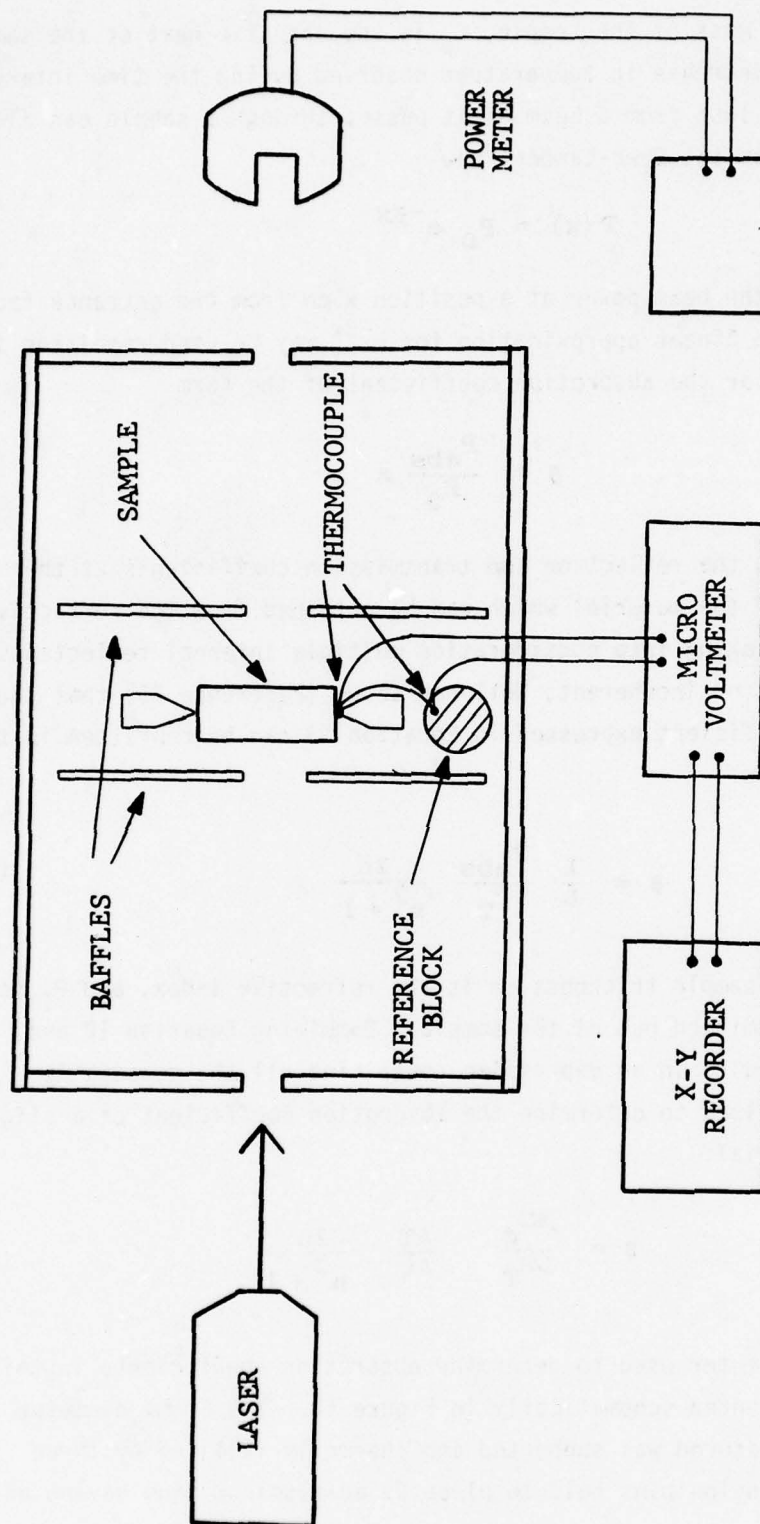


Figure 10. Schematic Diagram of Laser Calorimeter

inside diameter of 75 mm. A chromelalumel thermocouple was attached to the tip of one of the pins with indium solder permitting good thermal contact with the sample. This thermocouple was connected in series to another similar thermocouple imbedded in a large aluminum block which served as a constant temperature reference. The two thermocouples were so connected that when the reference block and the substrate were at the same temperature a null condition was produced resulting in a zero output voltage. When the sample was exposed to a laser beam of sufficient power, the energy absorbed by the sample resulted in a temperature rise indicated as a difference voltage. This voltage was applied to a Keithly Instruments Model 149 Milli-microvoltmeter providing a corresponding signal which in turn was displayed on a Mosley Model-7000A X-Y recorder as voltage (temperature) increase versus time. The power transmitted out of the sample was measured by a Coherent Radiation Model-201 power meter. Two large aluminum plates, each having a 30 mm diameter hole in its center to allow the laser beam to pass, were placed directly in front of and behind the sample to act as baffles to stray radiation. These baffles effectively shielded the sample thermocouple from any radiation reflected or diffracted to it which would have caused an erroneous output signal.

The sample, sample holder, baffles, and aluminum reference block were all contained in a plexiglass enclosure measuring 47.5 cm long, 31.5 cm wide and 29 cm high. Three 1.4 cm diameter holes were placed in the enclosure, two on the entrance side and one on the exit side, through which the incident, reflected, and transmitted beams passed. The absorption measurements were all made with a Korad KY-5 Nd:YAG laser having a 1.06 μm CW output rating of 200 watts multimode. However, the power levels used to obtain the calorimetric absorption measurements were never higher than 70 watts. The Nd:YAG laser uses dielectric stack reflectors designed for maximum reflection at 1.06 μm . The transmission through such stacks for radiation of other wavelengths can be appreciable and this permitted the use of a 1.8 mw 6328Å HeNe laser as a collinear alignment source. This provided a visible reference spot for repositioning of the substrates in the calorimeter before and after they had been coated.

The output from a typical calorimetry measurement is depicted in Figure 11 where the sequence of events can be observed from changes in the response curve. Prior to laser turn-on the flatness of the temperature vs time curve indicates that the sample has achieved a steady state temperature. Once the laser is turned on, absorption of radiation within the sample results in a linear temperature increase, terminating when the laser is turned off. The subsequent long term temperature decrease is indicative of the slow cooling of the sample as it returns to its initial steady state temperature. The abrupt increase and decrease of temperature observed respectively at laser turn-on and turn-off is caused by scattering of radiation from the surface of the sample directly to the recording thermocouple. In some respect this provides an indication of the optical quality of the surface finish.

The fact that the sample temperature is raised above the background temperature during the measurements requires that a correction be applied to account for the simultaneous cooling losses which occur during irradiation. This correction is obtained from the slope of the cooling curve after laser turn-off. The actual corrected absorption coefficient for the sample can then be obtained from the expression

$$\beta = \frac{m C_p}{L P_T} \left\{ \left. \frac{\Delta T}{\Delta t} \right|_{\text{heating}} + \left. \frac{\Delta T}{\Delta t} \right|_{\text{cooling}} \right\} \frac{2n}{n^2 + 1} \quad (16)$$

This same equation can be used for both an uncoated or a coated substrate provided the measurement is made with the coated surface positioned so that it faces the incident laser beam. In both of these cases, the transmission and reflection coefficients for the exit face remain the same.

The fractional amount of radiation absorbed within sample is $\beta \times L$. By making a calorimetric measurement first on an uncoated substrate and then on the same substrate after it has been coated, the amount of absorption which can be attributed to the coating alone (A_c) can be obtained from

$$A_c = \beta L_{\text{coated}} - \beta L_{\text{uncoated}} \quad (17)$$

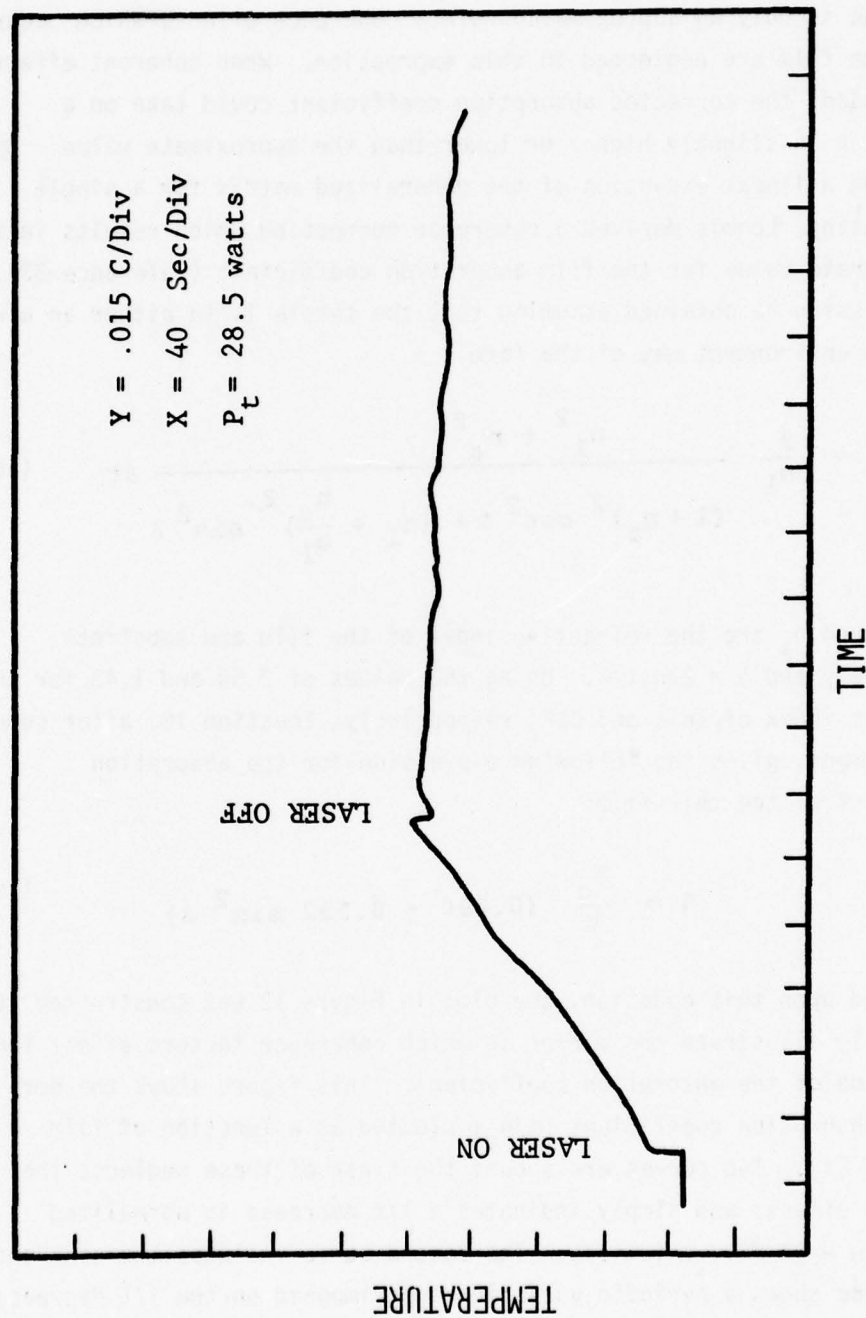


Figure 11. Output from Laser Calorimetry Measurement

By dividing A_c by the coating thickness (t), an approximate value for the absorption coefficient of the thin film coating is obtained. This value is only an approximation since coherence effects which occur within the film are neglected in this expression. When coherent effects are included, the corrected absorption coefficient could take on a value which is slightly higher or lower than the approximate value. By performing a linear expansion of the generalized matrix for a single layer coating, Loomis derived a coherence correction which results in a more accurate value for the film absorption coefficient (Reference 33). The expression he obtained assuming that the sample is in either an air or vacuum environment was of the form

$$A_c = \frac{2}{n_1} \frac{n_1^2 + n_s^2}{(1 + n_s)^2 \cos^2 \delta + (n_1 + \frac{n_s}{n_1})^2 \sin^2 \delta} \beta t \quad (18)$$

where n_1 and n_s are the refractive index of the film and substrate respectively and $\delta = 2\pi n_1 t / \lambda$. Using the values of 2.50 and 1.43 for the refractive index of ZnSe and CaF_2 respectively, Equation 18, after some rearrangement, gives the following expression for the absorption coefficient of the thin film:

$$\beta = \frac{A_c}{t} (0.890 + 0.532 \sin^2 \delta) \quad (19)$$

Based upon this equation, the plot in Figure 12 was constructed to graphically illustrate the manner in which coherence factors affect the calculation of the absorption coefficient. This figure shows the normalized absorption coefficient (β/A_c) plotted as a function of film thickness (t). Two curves are shown; the first of these neglects the coherence effects and simply indicates a $1/t$ decrease in normalized absorption with film thickness. The second curve includes the coherence effects and shows a periodic variation superimposed on the $1/t$ decrease. As can be determined from Equation 19, the approximate form for the absorption coefficient of ZnSe on CaF_2 (A_c/t) can, depending on film

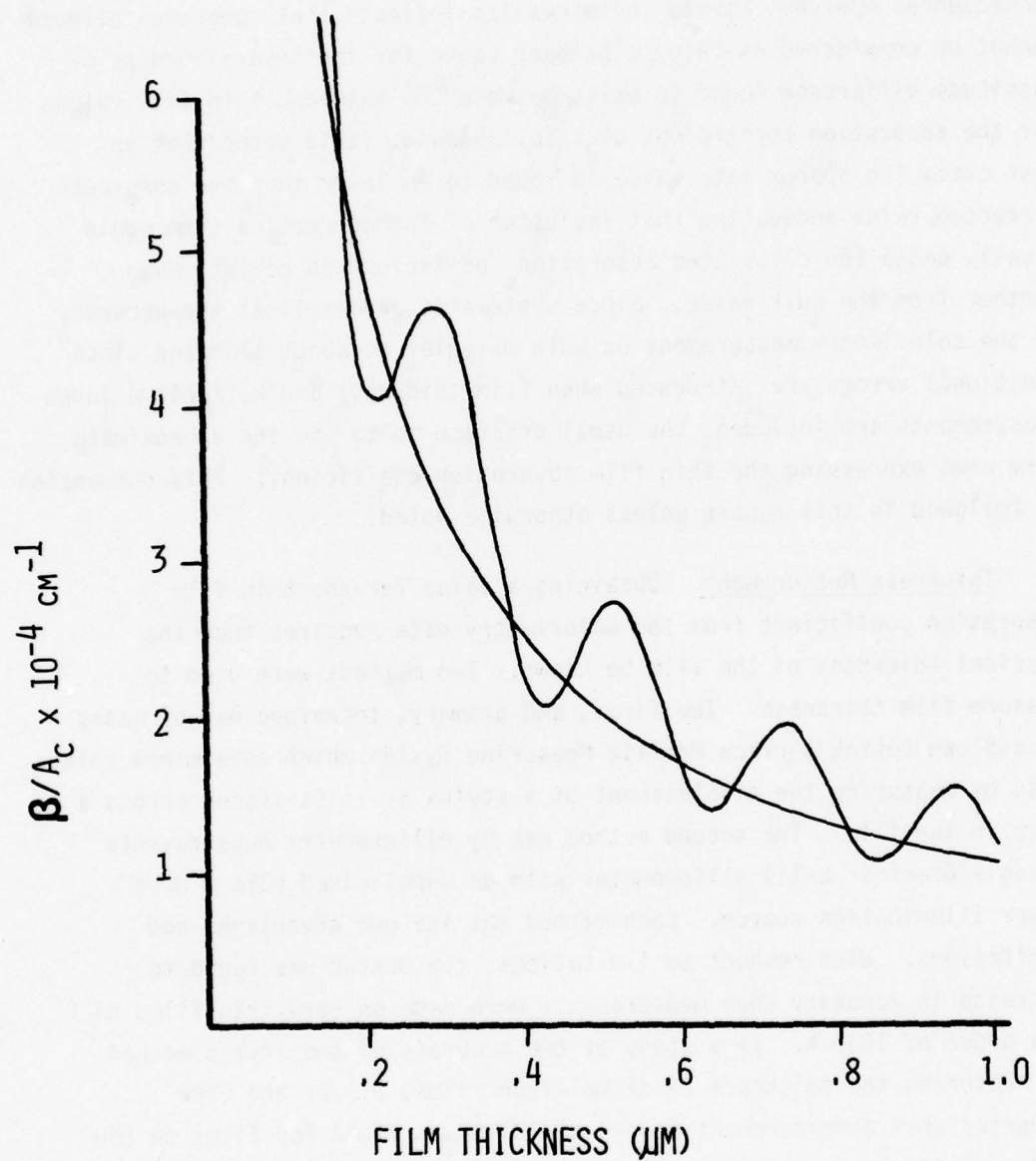


Figure 12. Normalized Coefficient of Absorption of a Thin Film Computed with and without Coherence Effects ($\lambda = 1.06 \mu\text{m}$, $n_{\text{film}} = 2.50$, $n_{\text{sub.}} = 1.43$)

thickness, give a value that in the worst case is a factor of 1.4 times lower than the coherence corrected value. From these observations two consequences emerge. First, these results indicate that coherence effects cannot be considered as being a primary cause for the several orders of magnitude difference found to exist between the bulk and thin film values for the absorption coefficient of ZnSe. Second, it is noted that in most cases the approximate value is found to be lower than the coherence corrected value indicating that inclusion of the correction term would usually cause the calculated absorption coefficient to deviate even further from the bulk value. Since systematic errors limit the accuracy of the calorimetry measurement on bulk material to about $\pm 10\%$ and since additional errors are introduced when film thickness and refractive index measurements are included, the usual practice is to use the approximate form when expressing the thin film absorption coefficient. This convention is followed in this report unless otherwise noted.

Thickness Measurement. Obtaining a value for the thin film absorption coefficient from the calorimetry data requires that the physical thickness of the film be known. Two methods were used to measure film thickness. The first, and primary, technique was by means of a Sloan Dektak Surface Profile Measuring System which determines thickness by measuring the displacement of a stylus as it is traced across a step in the film. The second method was by ellipsometry measurements using a Gaertner L-119 ellipsometer with an unpolarized 6328 Å HeNe laser illumination source. Each method has its own advantages and limitations. With respect to limitations, the Dektak was found to decrease in accuracy when measurements were made on very thin films of the order of 1000 Å. In a study of the accuracy of the stylus method of measuring the thickness of nickel-iron films, Silver and Chow reported that a measurement spread of 100 Å was found for films on the order of 400 Å thick while a 200 Å spread was observed for films nominally 3000 Å thick (Reference 34). In another study of this technique, Breitweiser indicated that the method has excellent precision, but that sample deformation can be produced which could affect the accuracy of the measurement (Reference 35). To obtain the best possible

accuracy in this program using the Dektak, thickness measurements were made at several different positions on the films and these values were then averaged.

In the case of thickness measurements obtained by using the ellipsometer, it is not so much the lack of accuracy that limits its use, but rather the fact that very lengthy and tedious steps are required to obtain a single measurement. In the course of this experimental investigation, both of these techniques were initially used; however, when it was determined that good agreement was being obtained between the resulting values, the ellipsometry method was discontinued. Consequently, only about half of the ZnSe films were evaluated by ellipsometry techniques.

Refractive Index. As part of the primary emphasis in this study to investigate the absorption coefficient of ZnSe thin films, measurements of the refractive index of all of the deposited coatings were made for the purpose of determining if any correlation existed between this optical constant and observed absorption variations. Several possible techniques were considered for measuring the refractive index of the thin films. Many of these have been well described by Heavens (Reference 36). Two of the techniques were employed in this study, ellipsometry and transmission spectrophotometry. As indicated previously, the ellipsometer measurements were made at a wavelength of 6328 \AA . Readings were made at two angles of incidence in the range of 60 to 75 degrees and refractive index and thickness values were calculated from data taken at each angle. The data reduction computations were made with the aid of a generalized computer program for the evaluation of ellipsometer data by McCrackin (Reference 37). Although ellipsometry offered a means of simultaneously obtaining two of the sought after parameters, refractive index and thickness, it did not provide these data at the same wavelength at which absorption measurements were being made. Transmission spectrophotometry, on the other hand, offered the capability of providing the refractive index at both the ellipsometer wavelength and at the absorption calorimeter wavelength provided that an independent thickness measurement was obtained. Consequently, both measurements were initially used in a complementary manner.

Transmission measurements were made with a Beckman DK-2 ratio recording spectrophotometer using a lead sulfide detector. With the beam at normal incidence, the transmission of the ZnSe coated CaF_2 substrates was measured throughout the wavelength range from 0.5 to 2.2 μm . Figure 13 shows the output of one of these measurements for a film 1.12 μm thick. For the specific case of a nonabsorbing film which has a refractive index greater than that of the substrate, the maxima in the transmission curve occur when the optical thickness (nt) of the film corresponds to an integral number of half-wavelengths. This is expressed by the relationship

$$\lambda_{\text{max}} = \frac{2nt}{m}, \quad m = 1, 2, 3, \dots \quad (20)$$

where n is the refractive index and t is the thickness of the film. Additionally, at these particular wavelengths the transmission of the film-substrate combination is the same as that of the uncoated substrate. The points of minimum transmission are found to be related by a similar expression of the form

$$\lambda_{\text{min}} = \frac{4nt}{2m+1}, \quad m = 0, 1, 2, \dots \quad (21)$$

By determining the positions of the turning points in the transmission curve and knowing the film thickness, Equations 20 and 21 can be used to obtain the refractive index of the film throughout the entire wavelength range included in the spectrophotometer measurement.

For the case indicated in Figure 13, which is typical of those obtained in this study, it can be seen that the values of maximum transmission for the coated substrate approach, but never actually equal that of the uncoated substrate; this is clearly evident at the shorter wavelengths. This deviation is due to the fact that the coating is not completely nonabsorbing and in fact becomes significantly absorbing at wavelengths close to the band edge for ZnSe. As is pointed out by Heavens, the inclusion of an absorption factor in the calculation of the transmission and reflection of an absorbing film on a transparent substrate involves some very complex expressions (Reference 38). Therefore, no simple relations of the form expressed in Equations 20 and 21 are

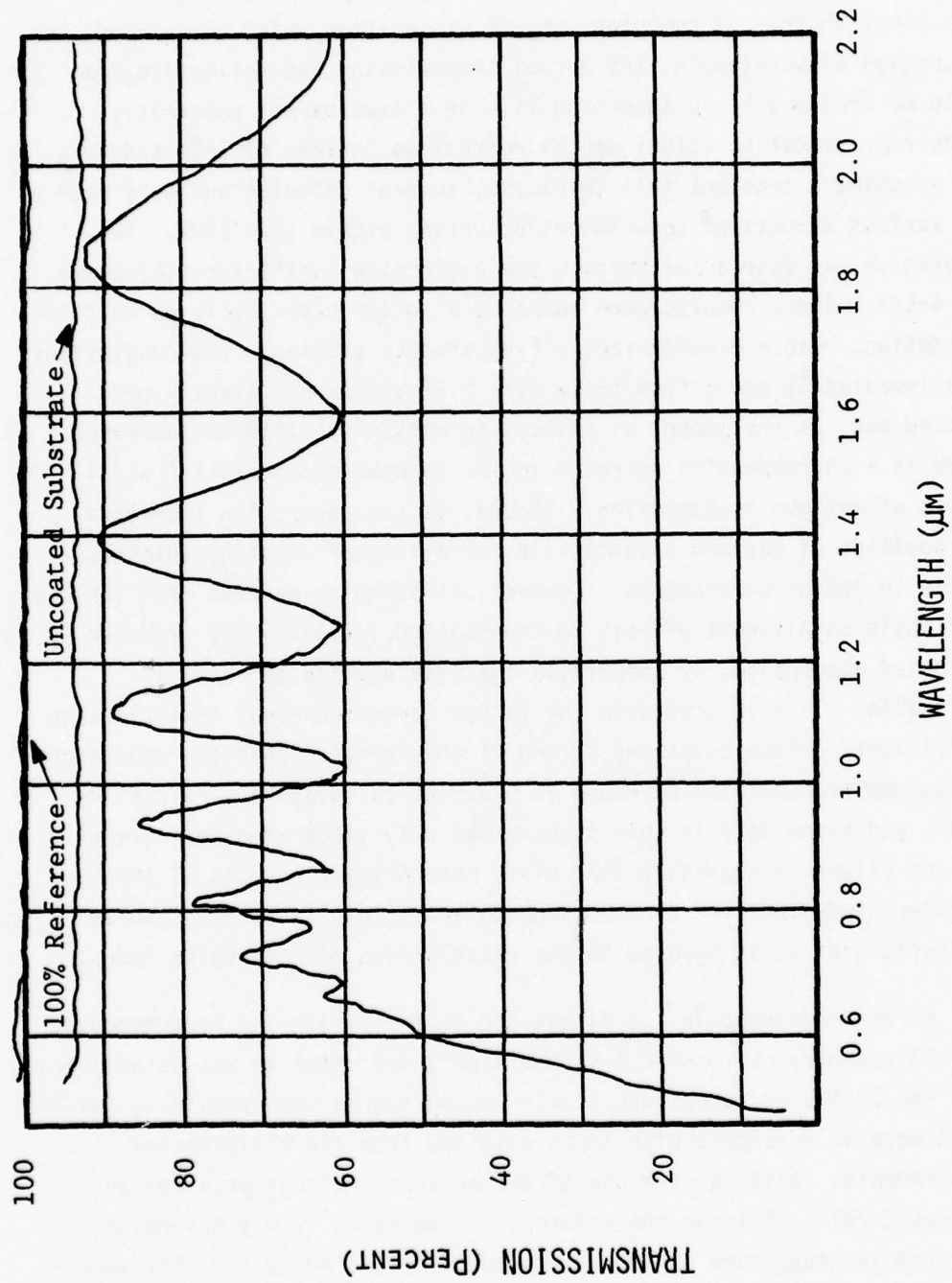


Figure 13. Typical Spectrophotometer Measurement of ZnSe Thin Film on a CaF₂ Substrate (t = 1.12 μm)

available for these cases. Consequently, it was desirable to determine how much error would be introduced into the refractive index calculations if the absorption were ignored and the simplified expressions used. To accomplish this, a computer program was written which calculated, as a function of wavelength, the actual transmission and reflection that would be produced by an absorbing film on a transparent substrate. Using representative values of the refractive indices of ZnSe and CaF_2 , and assuming a constant film thickness, several calculations were made for various amounts of absorptions occurring within the films. The absorption was introduced through the extinction coefficient (k) where $\beta = 4\pi k/\lambda$. These results were compared with the case involving no film absorption. Table 5 summarizes a typical case studied. Two conclusions were immediately drawn from these data. First, as has already been pointed out, as the amount of absorption within the film is increased, there is a corresponding decrease in the transmitted intensity at all points of maximum transmission. Second, as the absorption increases, the position of maximum transmission for a film of constant thickness shifts to longer wavelengths. However, it is quite evident from Table 5 that while significant effects on transmitted intensity are produced by increased absorption, by comparison the peak wavelength shift is negligible. This is true even for rather large increases in extinction coefficient. Since Equations 20 and 21 only require that the wavelength of maximum transmission be known in order to calculate the refractive index, and since data in this program was only taken when peak transmission values were greater than sixty percent, the results of the computer study indicate that no significant loss of accuracy results if the absorption is ignored in the calculations of refractive index.

As was mentioned in the discussion on film thickness measurements, the ellipsometry measurements were discontinued after it was established that the Dektak and spectrophotometry measurements were providing results which were in agreement with those obtained from the ellipsometry measurements. Although the use of two separate methods provided an increased reliability in the accuracy of the data, it was determined that the lengthy, time consuming procedures required by the ellipsometry technique did not warrant the redundancy of these measurements. This

TABLE 5
EFFECT OF ABSORPTION ON SPECTROPHOTOMETER MEASUREMENT OF
A THIN FILM

<u>Extinction Coefficient (k) *</u>	<u>Peak Transmission Intensity (%)</u>	<u>Peak Wavelength Position (Å)</u>
0	93.93	6400
0.001	91.62	6400
0.005	83.02	6400
0.010	73.59	6405
0.025	51.99	6410
0.050	30.16	6430

n(film) = 2.6

n(substrate) = 1.43

thickness = 9846 Å

$$* \beta (\text{cm}^{-1}) = 4\pi k / \lambda$$

decision was made only after many measurements had been completed on samples from several coating runs and it was demonstrated that consistent agreement of results was being achieved. Table 6 lists the results of the Dektak, spectrophotometry, and ellipsometry measurements made on an entire set of samples from one of these runs. Included is a comparison of refractive index calculations corresponding to a wavelength of 6328 Å as well as a comparison of the computed film thicknesses. The refractive index value shown in column A was obtained from spectrophotometry data and the average value of film thickness as determined by several Dektak measurements. This average thickness value is listed in column C. With the exception of one sample from this run, the refractive index and thickness results, as determined by ellipsometry measurements, show a range of acceptable values which satisfied the computer

TABLE 6
COMPARISON OF THICKNESS AND REFRACTIVE INDEX MEASUREMENT TECHNIQUES

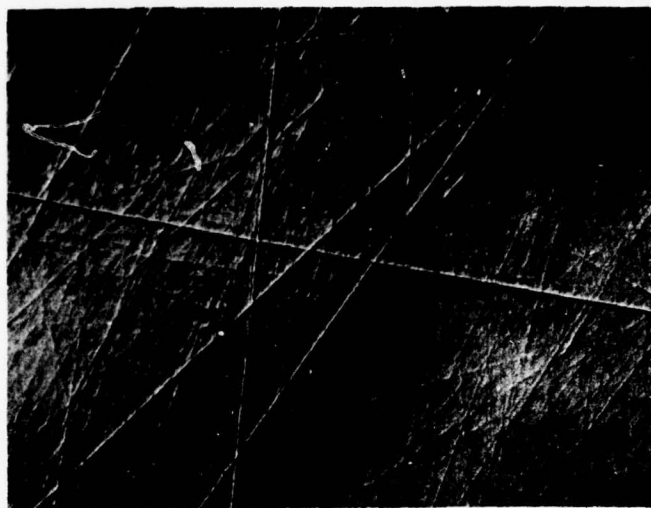
(A) Dektak and Spectrophotometer	Refractive Index		Thickness (μm)	
	(B) Ellipsometer (Angle of Incidence)	(C) Dektak	(D) Ellipsometer	
2.73	2.72-2.79 (70°) 2.72-2.79 (65°)	1.044	1.067-1.034 1.067-1.037	
2.72	* 2.68 (70°) (65°)	0.5925	*	0.6143
2.64	2.61-2.69 (70°) 2.62-2.68 (65°)	0.3073	0.3230-0.3112 0.3215-0.3124	
2.71	2.61-2.75 (70°) 2.61-2.75 (65°)	0.1440	0.1598-0.1482 0.1590-0.1470	

* Poor Sample Alignment - No Data

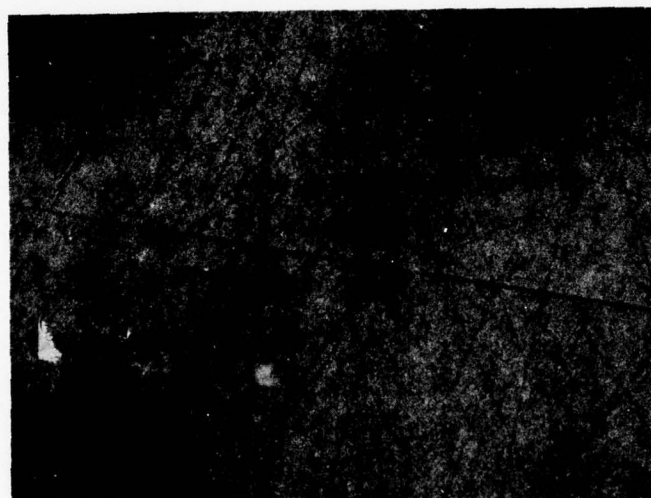
computations rather than one unique value. These values are listed in columns B and D respectively and are shown for measurements made at two separate angles of incidence. As is evident by this comparison, good agreement was achieved for both thickness and refractive index measurements obtained by the two techniques.

Surface Characterization. Because studies of absorption in bulk materials have revealed that surface preparation can significantly affect the absorption measurement (Reference 39), a means of qualitatively evaluating the substrate surface was incorporated into this program. Nomarski interference contrast microscopy was used to provide a technique for comparing the reproducibility of the substrate surface finish after repeated polishing. The Nomarski method offered a very sensitive technique for observing minute scratches, pits, or indentations on a reflecting surface to a degree not generally available with conventional or phase contrast microscopy. Figure 14 contains two micrographs which show the improvement over conventional microscopy that can be attained by using the Nomarski technique. Each micrograph encompasses the same area of a CaF_2 surface, but considerably more features are revealed in that obtained when the microscope was used in the interference contrast mode. Photomicrographs of each substrate were taken for every coating run in this program. These micrographs were then used to aid in determining if surface differences could explain any absorption variations which may have been observed in the same substrate after repeated polishing.

As part of the final evaluation of each coating, just prior to its removal from the substrate, a qualitative measure of the film adhesion was obtained. Two techniques were used. The first was similar to the adhesive tape test described in Military Specification MIL-M-13508C in which the sticky surface of a piece of cellulose tape is pressed onto the coated surface and then peeled off. Each film was then placed into either a pass or fail category depending on whether or not portions of the coating were removed from the substrate. The second technique was actually an adaptation of part of the procedure used to deliberately remove the film from the substrate prior to repolishing. This test



Nonmarski Micrograph



Conventional Micrograph

Figure 14. Comparison of Conventional and Nomarski Interference Contrast Micrographs of a CaF_2 Surface

involved the complete immersion of the coated substrate into a container of distilled water. In some cases this resulted in the immediate and complete crazing and delaminating of the films while in other cases only slight crazing or no effect at all was observed. It was noted that whereas many of the coatings "passed" the adhesive tape test, several of those that did pass were found to dramatically fail the immersion test. Since both of these tests were extremely qualitative, it was not known a priori what correlation could be inferred between a measured absorption level and a pass or fail condition. Nevertheless, since these tests were relatively easy to perform and could be made a part of the coating removal procedure, they were included as part of the final coating evaluation step.

Surface Analysis. Several analytical techniques were used to examine the coatings in an attempt to determine if chemical or structural differences were related to the observed absorption levels. Three areas of investigation were addressed by these techniques: crystalline structure, stoichiometry, and impurity content. The techniques applied to each of these areas are briefly described below.

Transmission electron microscopy was employed to perform electron diffraction analysis of the films for the purpose of noting differences in crystal structure which may have resulted from the different deposition conditions. This was the only one of the analytical techniques which could not be performed on the films deposited on CaF_2 substrates or on the witness plates. For these analyses only, the ZnSe films were deposited on copper electron microscope grids previously overcoated with a thin carbon film.

Since theoretical predictions and previous experimentation had both indicated that stoichiometric variations could result in increased infrared absorption within the coatings, a major emphasis was placed upon the identification of a method that could determine variations in stoichiometry. Five techniques were used to analyze the films. These five were x-ray fluorescence, electron microprobe, Auger electron spectroscopy (AES), electron spectroscopy for chemical analysis (ESCA),

and Rutherford backscattering (RBS). The AES and ESCA techniques were used in conjunction with Argon ion sputtering providing a capability for conducting profile analyses of the coatings. No attempt will be made to describe these surface analysis techniques in detail since a number of references exist which do this quite adequately (e.g., References 40, 41). Mention should be made, however, of the capability of each method as it applies to the problem of determining film stoichiometry. Unfortunately, very little data is available which describes each instrument's ability to detect small deviations of one of the major constituents of a material from a truly stoichiometric composition. Rather, what is most often presented is the instrument's detection limit, that is, the smallest atomic fraction of an impurity material that can be detected in a host material of different composition. Although this is not the sensitivity limit which defines the ability to detect excess Zn in a ZnSe crystal, for lack of a better means of defining stoichiometric sensitivity, this number can reasonably be assumed to be a lower limit for such a case. Table 7 summarizes the published sensitivities for each of the techniques.

TABLE 7
SURFACE ANALYSIS SENSITIVITIES

<u>Technique</u>	<u>Sensitivity (Atomic Fraction)</u>	<u>Reference</u>
AES	10^{-3}	42
RBS	$10^{-1} - 10^{-4}$ (Depends on Atomic No.)	42
ESCA	$10^{-2} - 10^{-3}$	42
Electron Micro- probe	- 0.01 (Stoichiometry Deviation)	43

Not listed in Table 7 is the x-ray fluorescence technique. Gilfrich has pointed out that there is no great abundance of references which describe its use in surface characterization (Reference 44). As a consequence, the sensitivity of the technique had to be determined before a decision on its applicability could be made. To do this, a glass microscope slide was coated with ZnSe and cut into several 0.5 cm x 0.5 cm pieces for x-ray fluorescence analysis. After being corrected for background effects, the ratio of the total number of observed counts in the Zn peak to those in the Se peak during a 100 second analysis was determined for four of the coated pieces. Since the analyses were performed on the same film, this experiment was designed to give the statistical variability of a single analysis which essentially would place a lower limit on the detectability of the Zn to Se ratio. Table 8 gives the results of these measurements and includes the effects of two separate background measurement corrections. The Zn/Se ratio is uncorrected for

TABLE 8
X-RAY FLUORESCENCE SENSITIVITY

<u>Sample No.</u>	<u>Background Correction Used *</u>	<u>Zn/Se (count ratio)</u>
2	First	1.169
2	Second	1.143
3	First	1.168
4	First	1.167
5	First	1.158
5	Second	1.154
Average		1.160
Deviation		0.010

* Two separate measurements for background effects were made.

actual atomic ratio and only represents the observed x-ray counts. These results, which show a statistical deviation of slightly less than 1%, indicated that the x-ray fluorescence technique had a capability comparable to the other techniques being considered.

As was discussed in the previous section, the theoretical models for predicting absorption in the coating indicated that the absorption levels observed in the ZnSe films could be explained by the presence of fractional excesses of Zn in amounts of approximately 10^{-3} or less. This value borders on the state-of-the-art detectability limits of all the techniques and it was for this reason that the five separate techniques were utilized. Although it was expected that one or more of the methods might prove to be inadequate, it was also felt that at least one, or several in conjunction, would provide sufficient data to make a positive conclusion concerning stoichiometric variations in the coatings if any existed.

The final surface analysis techniques to be performed on the coatings were those for the detection of impurities other than Zn or Se. Scans for elements with atomic number greater than 3 were made using the AES, ESCA, and electron microprobe techniques already mentioned. The sensitivity limits for detecting impurities by each of these techniques are those listed in Table 7.

SECTION IV

RESULTS AND DISCUSSION

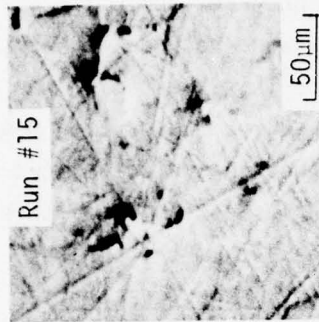
1. SURFACE AND INTERFACE EFFECTS

In attempting to identify the causes for the abnormally high infrared absorption in ZnSe coatings, two principal areas had to be investigated. The first of these involved sources of absorption which originated from either film surface effects or coating-substrate interface effects. The second concerned sources of absorption existing within the coating material itself. The fact that surface and interface effects deserve consideration is reflected in the high degree of emphasis which is presently being placed on the development and improvement of surface finishing techniques for bulk materials used as infrared optical components. These efforts have shown that a significant portion of the infrared absorption in polished bulk material originates at the surface and that surface finishing techniques can measurably change these values (Reference 39). There has been speculation that the high level of absorption observed in measurements of coated substrates may have been due, in part, to an enhancement of substrate surface absorption when the coating was deposited on the substrate. To evaluate the significance of this factor in this research program, it was first necessary to determine if the substrate polishing procedures being used were creating any large variability in surface absorption from sample to sample. If this were found to be so then it would be necessary to determine if any correlation could be made between absorption measured in the coated substrate and the initial substrate surface absorption.

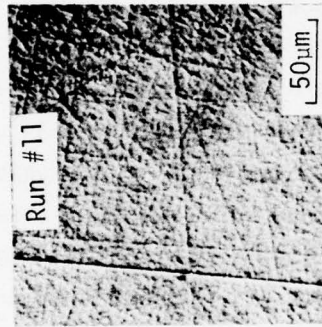
At present there exists no technique which can accurately separate bulk absorption values from surface absorption values in a single substrate. This fact presents difficulties in trying to assess the effects of substrate surface absorption on measured coating absorption. Nevertheless, with the numerous substrates used in this study, enough characterization data was obtained to allow inferences to be made concerning this effect. By means of the combined results obtained from the Nomarski micrographs taken of each polished substrate and the uncoated substrate absorption measurements, an evaluation of the polishing

procedure was possible from which the significance of surface and interface absorption was determined. Two findings emerged from the characterization study. First, the micrographs revealed that the substrate surface features for the same substrate were not always the same from one polishing to the next. However, perhaps more significant is the fact that although definite differences in total absorption were observed between different substrates, very little difference was noted for any one substrate when comparisons after repeated coating and repolishing runs were made. This was found to be true in spite of the fact that the physical appearance of the surface had obviously been altered.

Figure 15 shows the surface characteristics along with the measured $1.06 \mu\text{m}$ absorption coefficients for two CaF_2 substrates (No. 12 and 27) used in this study. The absorption and Nomarski measurements were made after six separate polishing runs, three for each substrate. Each substrate had been coated with ZnSe between each individual run and the coating subsequently removed. The fact that any measurement of Sample No. 27 when compared with any measurement of Sample No. 12 shows a factor of about four times the amount of absorption independent of surface finish clearly indicates that the difference is due to material properties rather than surface properties. The slight variation observed among the measurements made on any one sample could represent differences due to surface finish. However, since the error in the calorimetry measurement is on the order of 10% and since this error increases once absorption levels on the order of 10^{-5} cm^{-1} are approached, assigning the cause for these variations to differences in surface finish cannot be done with high confidence. Nevertheless, this study did indicate that within measurement error the polishing procedures used did produce results which were repeatable from the point of view of continually attaining the same total absorption level in any particular substrate. No correlation could be made, however, between surface appearance and uncoated substrate absorption level, nor could any correlation be made between surface appearance and coated substrate absorption when these values were associated with the corresponding Nomarski micrographs.

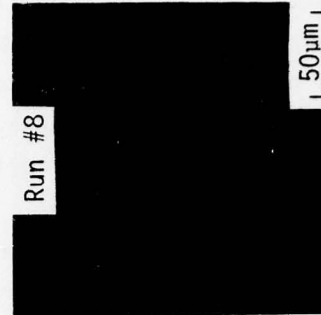


$$\beta = 0.8 \times 10^{-4}$$

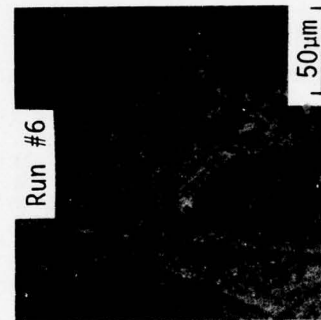


$$\beta = 1.4 \times 10^{-4}$$

SAMPLE NO. 12

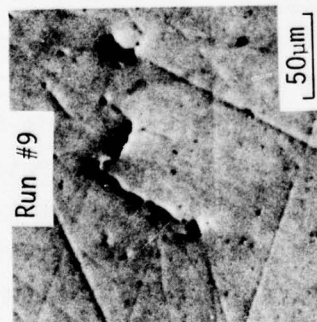


$$\beta = 4.8 \times 10^{-4}$$

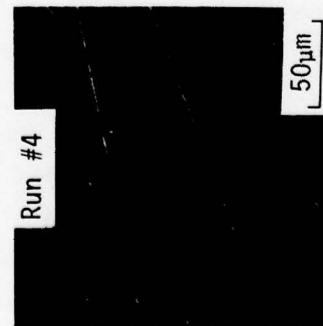


$$\beta = 5.5 \times 10^{-4}$$

SAMPLE NO. 27



$$\beta = 1.0 \times 10^{-4}$$



$$\beta = 4.5 \times 10^{-4}$$

Figure 15. Variation of Substrate Surface Features and Infrared Absorption Coefficient After Repeated Optical Polishing

The conclusion which was drawn from these data tended to indicate that the large variations in coating absorption which were observed under different deposition conditions in this program, and which will be discussed later in this section, most probably were not due to the slight differences noted in the substrate absorption. This indication was confirmed to a much greater degree by data obtained from absorption measurements made on ZnSe coatings of different thicknesses, but deposited under identical deposition conditions. As described in Section II of this report, each of the four CaF_2 substrates in the vacuum chamber was sequentially exposed to the ZnSe vapor stream by means of a shutter system. This resulted in the production of four different thicknesses of ZnSe coatings during each coating run. The absorption value, as defined by Equation 17, obtained on each of these coatings, was plotted against the corresponding measured film thickness. A linear least squares fit was then made to these data from which a determination of both the coating absorption coefficient and the extent of surface and interface absorption could be made. This is directly analogous to the technique used to separate the values of internal absorption from surface absorption in measurements made on bulk material (Reference 45). In these cases measurements are made on several bulk crystals of different thicknesses, all of which were cut from the same large piece and then polished in an identical manner. When the resulting calorimetry data for each crystal are plotted as total absorption versus sample thickness, the slope of the line representing the linear fit to these data gives the internal or bulk absorption coefficient while the intercept represents the zero thickness or surface contribution to the absorption. An example of some results obtained from one of these measurements performed on a piece of bulk polycrystalline KCl is shown in Figure 16. It should be noted that the actual data points deviate somewhat from the linear fit. This is due, in part, to the inaccuracies in the precision of the calorimetry process, which for bulk material is normally considered to be about 10%. The results obtained using this same analysis technique on different thicknesses of ZnSe films from three separate coating runs are shown in Figure 17. The three cases shown represent the highest and lowest absorption levels observed in this study as well as one intermediate

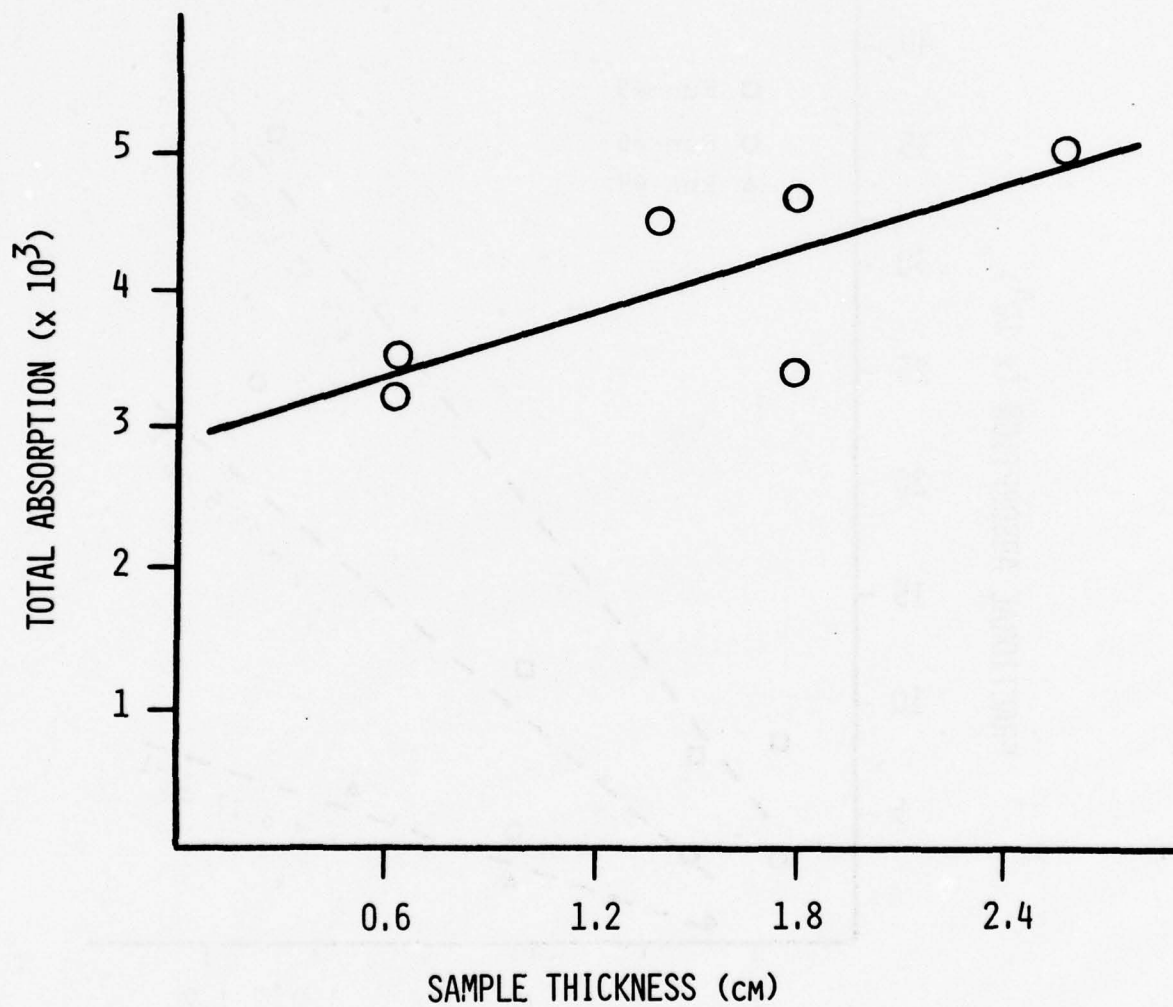


Figure 16. 10.6 μm Optical Absorption vs Sample Length for a KCl Crystal. (From Ref. 56)

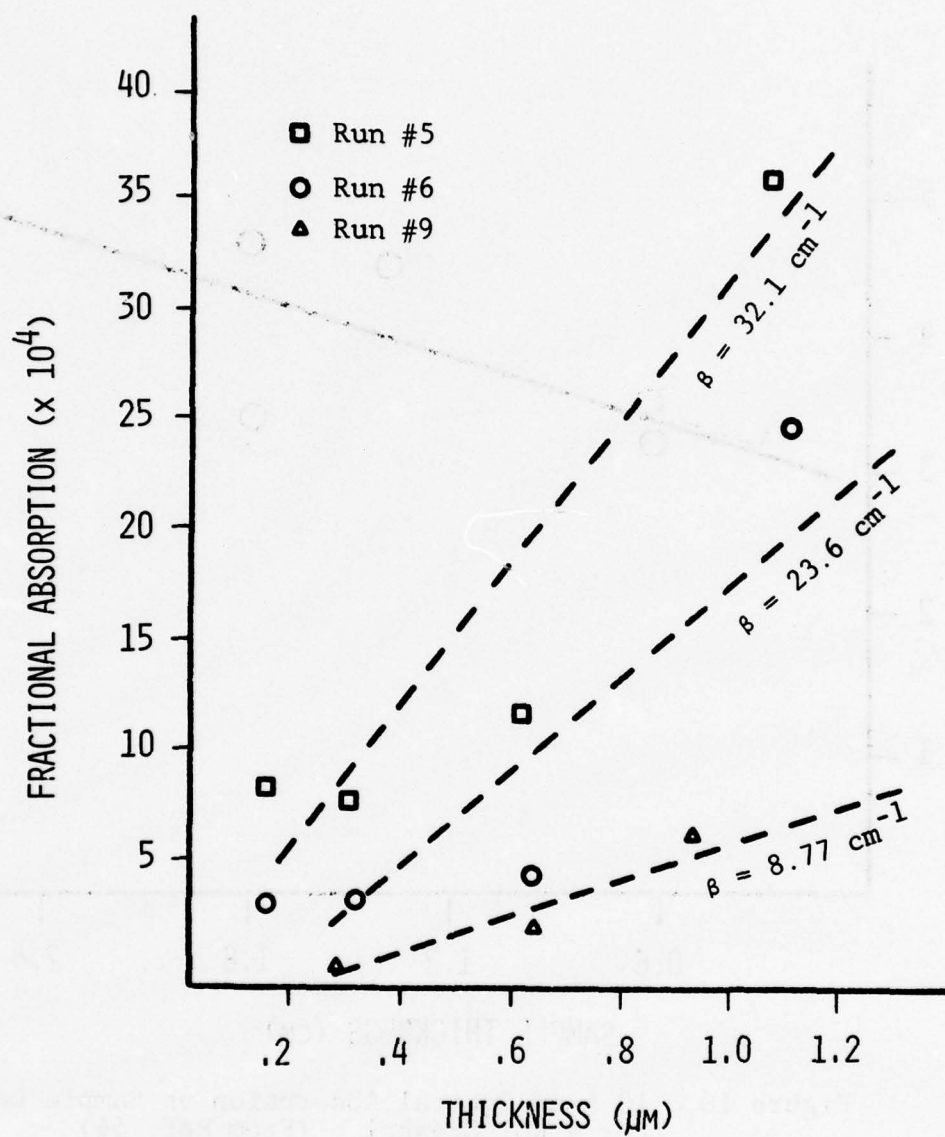


Figure 17. Absorption Change with Film Thickness.

value. The interpretations which can be drawn from these three data sets also apply to the data from all other coating runs not included in this plot. These additional data have been deliberately omitted to allow clear interpretation of the trends depicted in the figure.

The trends are indicated in the figure by dashed lines. By including these trend lines, it was possible to estimate a value for the absorption coefficient associated with each deposition run. These values are also indicated on the plot. It is noted that the trend of decreasing absorption with decreasing film thickness existed regardless of whether the coating was characterized as being highly absorbing, $\beta = 32 \text{ cm}^{-1}$, or of lower absorption, $\beta = 8.8 \text{ cm}^{-1}$. In addition, it is seen that the absorption value as the film approaches zero thickness is quite small in comparison to the level of absorption indicated by the calculated film absorption coefficient. The existence of this low level of absorption at the zero thickness point does support the possibility of some small contribution to the overall absorption due to surface or interface effects. However, accurate interpretation of these finite absorption values for very thin films ($< 2000 \text{ \AA}$) is confounded somewhat by two factors. First, as previously mentioned, even for the case of measurements on bulk material, the precision of the calorimetry measurement is only about $\pm 10\%$. This precision becomes considerably less when the film absorption is calculated by determining the difference between the absorption measured in an uncoated and a coated substrate. Additionally, this precision is decreased even further as either the measured absorption decreases or as the film thickness decreases. Second, as previously described, the coherence effects in thin films are expected to cause the measured absorption to deviate from the straight-line approximation by the amount that depends upon both the film thickness and its refractive index.

Despite the difficulties that exist in evaluating data measured on the thinnest of the films, it is still possible to conclude that the predominant amount of infrared absorption measured in these ZnSe coatings is attributable to absorption within the film rather than absorption on the surface or at the interface.

2. ABSORPTION WITHIN THE COATING

With the above data having shown that the surface and interface effects were not the most significant factors, particularly for thicker films, the second area of investigation could then be addressed, that area being related to absorption within the bulk of the thin film coatings. Since experimental results from past investigations had given strong support to the hypothesis that stoichiometric variations were responsible for high absorption within the ZnSe films, the major portion of this experimental effort was directed toward investigating this factor. The Gunther theory describing the growth of binary compounds, which has already been described, provided an ideal means for determining whether or not variations in the stoichiometry of the ZnSe films were affecting the absorption. This theory predicted that the film stoichiometry could be affected by three deposition parameters: substrate temperature, deposition rate, and Zn to Se vapor flux ratio. Therefore, experimental coating procedures were designed to provide a means of relating coating absorption to changes in each of these deposition parameters. The results were then correlated to predictions based upon the Gunther theory.

The first aspect of the theoretical description which was examined concerned effects due to differences in substrate temperature. According to the Gunther theory, depositions onto substrates heated to a high temperature are more likely to result in a stoichiometric coating than depositions onto an unheated or only slightly heated substrate. The means of confirming this for the case of ZnSe deposited onto CaF_2 appeared quite simple, that is, depositions at a constant flux rate were to be made onto substrates heated to different temperatures. This would be followed by a comparison of the infrared absorption levels measured in each of the ZnSe coatings. If stoichiometric deviations induced corresponding absorption deviations, then the coatings deposited at lower substrate temperatures could be expected to exhibit the higher levels of absorption. In fact, additional material properties made this comparison quite difficult. The problem encountered was related to the mismatch in thermal expansion coefficient between ZnSe and CaF_2 .

Table 9 lists the thermal expansion coefficients for four materials commonly used in the fabrication of infrared optical components. A significant difference is seen to exist between the thermal expansion coefficient of ZnSe and those of CaF_2 and KCl. Because of this difference, ZnSe when deposited onto these materials held at high temperatures will become highly stressed when the temperature is reduced to room temperature values. If these stresses are sufficiently high, the coating will often craze or crack and become detached from the substrate. As evident from the data in Table 9, this has become a significant problem, particularly with respect to ZnSe coatings on KCl laser windows. The difficulties of the mismatch with respect to CaF_2 are not as serious as those with KCl; however, this factor did affect the attempts in this program to experimentally verify the predictions of the Gunther theory with respect to substrate temperature effects.

TABLE 9
THERMAL EXPANSION COEFFICIENTS OF INFRARED MATERIALS AT 300°K

<u>Material</u>	<u>$\alpha \times 10^6 (\Delta l/l)$</u>	<u>Reference</u>
ZnSe	7	46
GaAs	7	47
CaF_2	18	46
KCl	37	47

High and low substrate comparisons were attempted, nevertheless, for three different rates of deposition. The results of these comparisons are summarized in Table 10, which shows the deposition rate, substrate temperature, and measured absorption for each set of coated samples. The last column in this table lists a comment relating to whether or not film crazing occurred when the samples were cooled to room temperature and removed from the vacuum chamber. For the two cases where the

TABLE 10
COMPARISON OF COATINGS DEPOSITED AT
HIGH AND LOW SUBSTRATE TEMPERATURES

<u>Run No.</u>	<u>Rate (Å/sec)</u>	<u>Substrate Temp. (°C)</u>	<u>A_c/t (cm⁻¹)</u>	<u>Condition</u>
9	0.9	76	5.5	Intact
11	0.9	181	6.3	Crazed within 24 hrs
7	3.6	67	9.3	Intact
16	2.1	255	No Data	Crazed Immediately
4	17.0	22	29.4	Intact
3	14.0	75	30.7	Intact

substrate temperature was substantially increased, the absorption measurements were either not possible due to immediate crazing or were affected by the fact that partial crazing had occurred prior to completion of the absorption measurement. When it was determined to be impossible to successfully carry out a comparison of absorption in coatings deposited at elevated substrate temperatures, further attempts were made to accomplish a similar comparison between films deposited onto room temperature substrates and substrates which were only slightly heated. No difference due to substrate temperature was found for this case. It was concluded that the small difference in substrate temperature for the latter case was not sufficient to adequately demonstrate the effects due to stoichiometry which were predicted by the Gunther Theory.

As a consequence of the difficulties which resulted from the mismatch in the thermal expansion coefficients of ZnSe and CaF₂, it was not possible to verify the expected results relating coating absorption and substrate temperature. However, in a somewhat related study which involved vapor-phase epitaxial growth of ZnSe on GaAs, Yim and Stafko

found that substrate temperature had a significant effect on film stoichiometry and, in fact, as theory would predict, the optimum growth conditions for films grown on substrates heated to temperatures between 650°C and 890°C were found to occur for the high, 890°C, case (Reference 48). Even in this case, where Table 9 shows that a rather good thermal match exists between ZnSe and GaAs, it was found that slow cooling was required to prevent the films from cracking.

Although the experimental studies to determine the effect of substrate temperature on infrared absorption within the films proved inconclusive, this was not the case involving investigations of the effects of deposition rate. Again based upon the Gunther theory, it was expected that at a fixed substrate temperature and with the flux rate of each component being equal, optimum conditions for obtaining stoichiometric films would occur when low deposition rates were used. Accordingly, absorption within the films, if due to nonstoichiometry, would be expected to display a decreasing trend as the deposition rate was lowered.

To experimentally determine if this behavior were true for ZnSe, several depositions were made at rates which ranged between 0.9 and 35 Å/sec. All of these depositions were made onto CaF_2 substrates which were heated to temperatures within the range of 67 to 80°C with the average temperature being 74°C. This value was selected as being the highest temperature at which integrity of the coating could be maintained, but which also provides a heated surface which would result in a decreased probability of having condensable impurities deposited in the films.

In addition to the calorimetric absorption measurements, refractive index measurements were made on each of the coatings deposited in this portion of the experimental investigation. This was done with the intent of using deviations of the film refractive index from that of the bulk crystal value as a possible indicator of nonstoichiometry. The accuracy of these refractive index measurements is affected by that of the film thickness measurement, and since this accuracy is highest for

the thicker films, only those coatings from each deposition run which were nominally 1 μm or greater in thickness were used in the comparison of refractive indices. The selection of the data associated with the thicker films also provided more data points since there were more maximum and minimum points in the spectrophotometric transmission curves than would have been the case with the thinner coatings. The results of these measurements are shown in Figure 18 for deposition rates which were varied from a low of 0.9 $\text{\AA}/\text{sec}$ to a high of 35 $\text{\AA}/\text{sec}$. The refractive index within the wavelength range of 0.6 to 1.6 μm is shown for four of these coating runs along with the value for bulk ZnSe. Each of the four sets of data has been fitted to a third degree polynomial by a least squares analysis and this is shown in Figure 18 as a dispersion curve for each of the cases. Each of the data points shown in Figure 18 was obtained using the spectrophotometric technique in which the refractive index is obtained either from

$$n = \frac{m\lambda}{2t} \quad m = 1, 2, 3, \dots \quad (22)$$

for wavelengths corresponding to a maximum in the transmission scan or from

$$n = \frac{(2m + 1)\lambda}{4t} \quad m = 0, 1, 2, \dots \quad (23)$$

for wavelengths corresponding to a minimum. All points associated with a particular dispersion curve are seen to depend on the same value of film thickness, and, correspondingly, the error associated with the thickness measurement will affect each point identically. This, in effect, defines an error value applicable to the entire dispersion curve. A measure of this error is included in Figure 18 for each of the curves and is shown as an error bar along with an equivalent percent variation.

It was found that the error associated with each of the curves was too large to allow an accurate comparison of the refractive index for films produced at deposition rates which were not widely separated in magnitude. However, a comparison of extreme cases revealed that an overall trend did exist indicating that lower deposition rates tended to

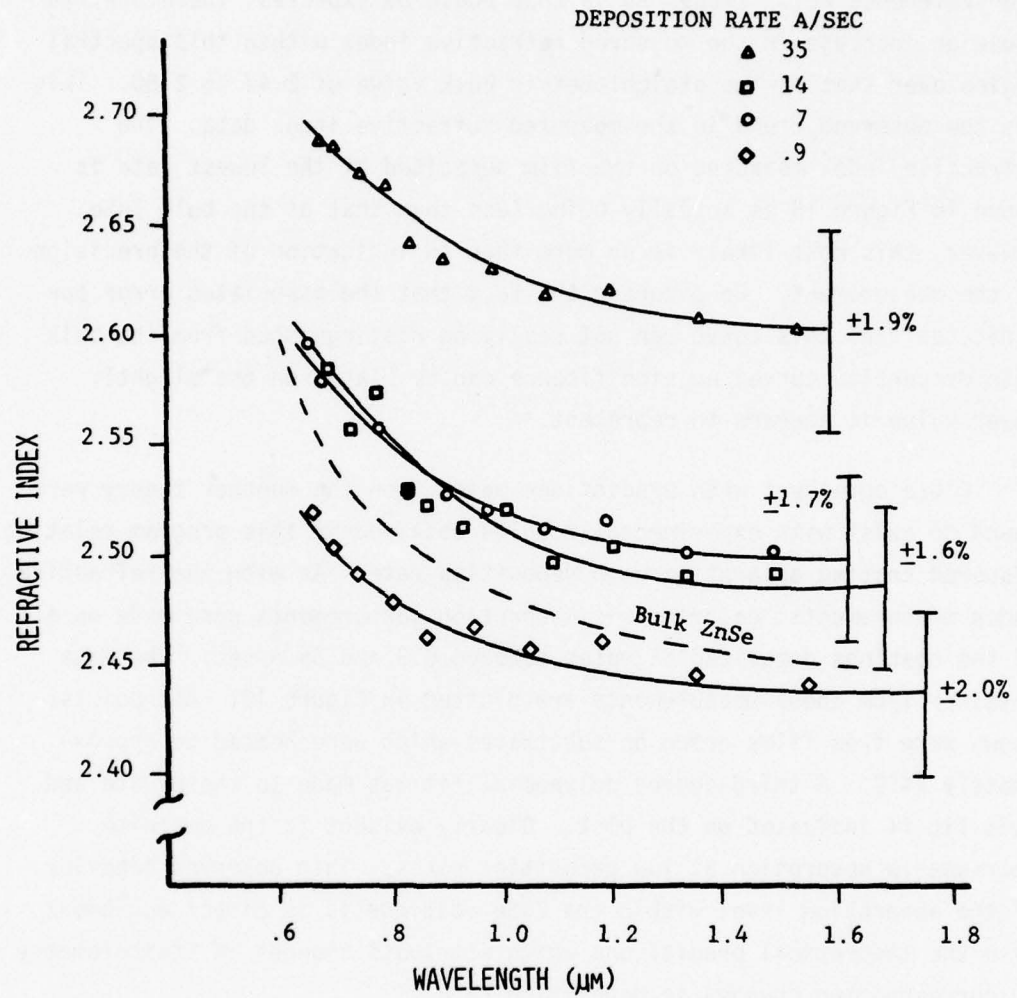


Figure 18. Effect of Deposition Rate on Refractive Index.

produce a coating having a refractive index which approached that of the bulk index. Yarovaya et al. have measured the refractive index of metallic Zn and found that it undergoes an anomalous dispersion in the near infrared region of the spectrum where it increases to a value greater than 5.0 (Reference 26). Excess Zn in ZnSe would be expected, therefore, to cause an increase in the measured refractive index within this spectral region over that of the stoichiometric bulk value of 2.47 to 2.60. This was the observed trend in the measured refractive index data. The refractive index measured on the film deposited at the lowest rate is shown in Figure 18 as actually being less than that of the bulk ZnSe. However, this most likely is no more than an indication of the precision of the measurement. Considering the fact that the associated error bar indicates that this curve can not really be distinguished from the bulk ZnSe dispersion curve, no significance can be placed on the slightly lower value it appears to represent.

Close agreement with predictions based upon the Gunther theory were found to exist with experimental results obtained in this program relating measured coating absorption with deposition rate. As with the refractive index measurements, calorimetric absorption measurements were made on all of the coatings deposited at rates between 0.9 and 35 Å/sec. The data obtained from these measurements are plotted in Figure 19. All points shown were from films grown on substrates which were heated to approximately 74°C. A third-degree polynomial fit was made to these data and this fit is indicated on the plot. Clearly evident is the definite decrease in absorption at low deposition rates. This observed behavior of the absorption level within the ZnSe coatings is in direct agreement with the theoretical predictions which attribute changes in stoichiometry to corresponding changes in deposition rate.

Since the electron beam evaporations were all made using a source material that was in the form of bulk crystalline ZnSe, all the depositions previously discussed were carried out with the flux rates of Zn and Se being equal. However, since Zn and Se have widely different vapor pressures, an opportunity existed to investigate the third hypothesis based upon the theoretical description of binary component evaporation.

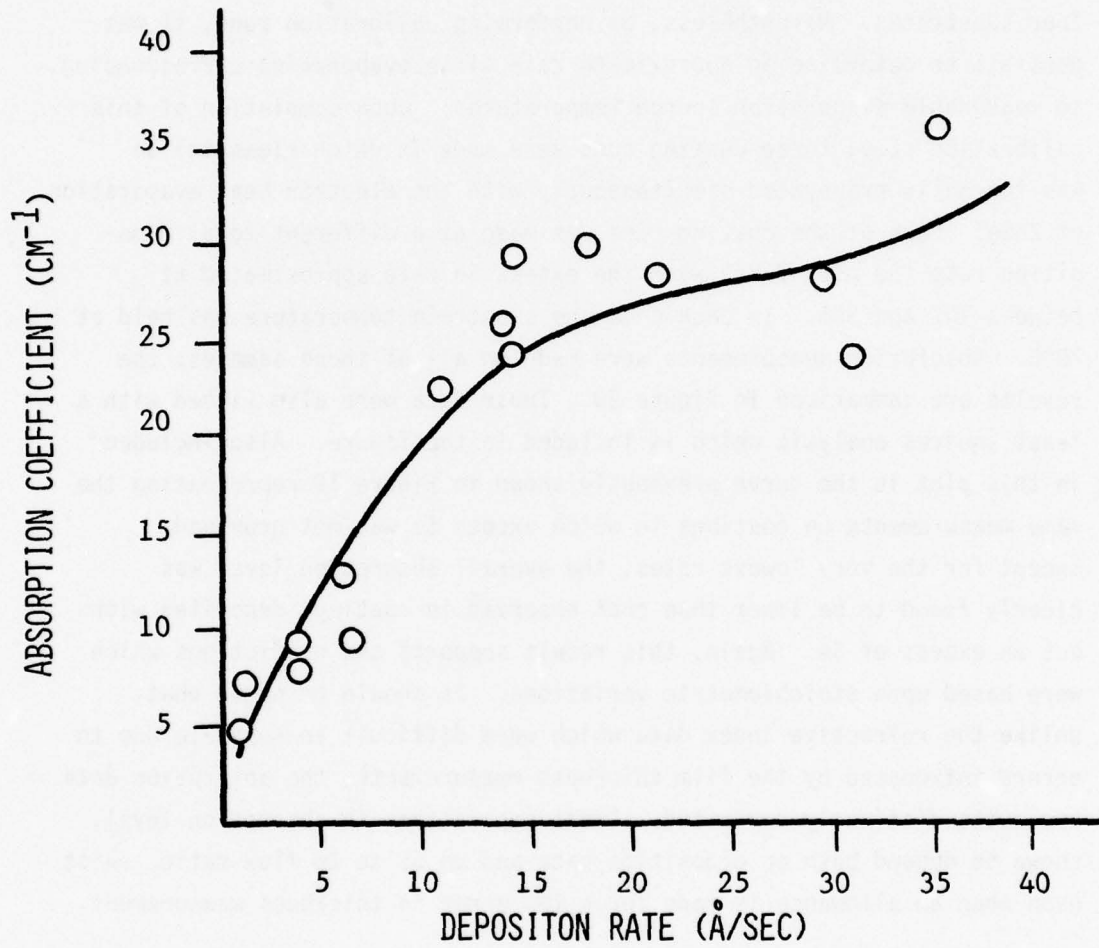


Figure 19. Effect of Deposition Rate on ZnSe Film Absorption at 1.06 μm .

This hypothesis indicated that the introduction of an excess of the more volatile component (Se) into the evaporant stream would increase the probability for producing a more nearly stoichiometric film and, consequently, result in lower absorption levels. To accomplish this, a resistance heated Se evaporation source was added to the vacuum chamber. Because this source could not be centrally located in the system, geometric factors prevented the same Se deposition rate onto each of the four substrates. Nevertheless, by performing calibration runs, it was possible to determine an approximate rate of Se evaporation corresponding to measurable evaporation source temperatures. Upon completion of this calibration step, three coating runs were made in which elemental Se was thermally evaporated simultaneously with the electron beam evaporation of ZnSe. Each of the coating runs was made at a different total deposition rate (Se plus ZnSe) with the excess Se rate approximated at between 10% and 30%. In each case the substrate temperature was held at 70°C. Absorption measurements were made on all of these samples; the results are summarized in Figure 20. These data were also fitted with a least squares analysis which is included in the figure. Also included in this plot is the curve previously shown in Figure 19 representing the same measurements on coatings in which excess Se was not provided. Except for the very lowest rates, the overall absorption level was clearly found to be lower than that observed in coatings deposited without an excess of Se. Again, this result supports the predictions which were based upon stoichiometric variations. It should be noted that, unlike the refractive index data which were difficult to separate due to errors introduced by the film thickness measurements, the absorption data are quite distinctly separated. These separations in absorption level, shown to depend both on deposition rate and on Se to Zn flux ratio, exist even when an allowance is made for a 10% error in thickness measurement.

3. STRUCTURAL AND CHEMICAL ANALYSIS

As a means of independently verifying that stoichiometric variations existed in ZnSe films deposited at different rates, several state-of-the-art surface and chemical analysis techniques were applied to the coatings. As stated in the previous section describing these techniques, theoretical estimates of the expected stoichiometric deviations indicated that, for

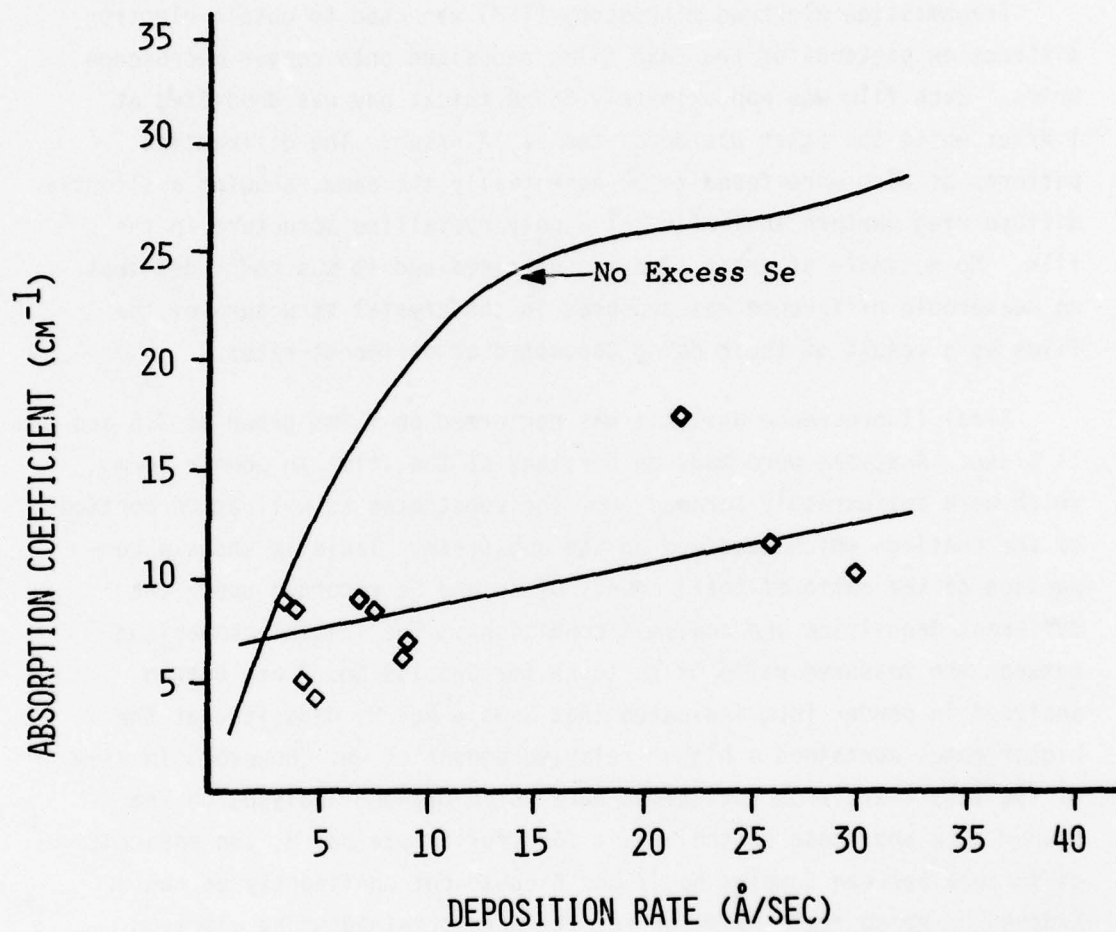


Figure 20. Effect of Excess Se on ZnSe Film Absorption at $1.06 \mu\text{m}$.

the applications to which these techniques were applied in this program, most of them would be at the limits of their detection capabilities. For this reason it was not unexpected that somewhat incomplete results were obtained in several of the analyses. The results of each analytical technique which was employed will be discussed, however, since the combined results, when evaluated and compared, did provide a useful set of data.

Transmission electron microscopy (TEM) was used to obtain electron diffraction patterns of two ZnSe films deposited onto copper microscope grids. Each film was approximately 500 Å thick; one was deposited at 1 Å/sec while the other was deposited at 17 Å/sec. The diffraction patterns of each were found to be essentially the same, showing a slightly diffuse ring pattern indicative of a polycrystalline structure in the film. No estimate of grain size was obtained and it was concluded that no measurable difference was produced in the crystal structure of the films as a result of their being deposited at different rates.

X-ray fluorescence analysis was performed on films grown at 3.5 and 11 Å/sec. Analyses were made on portions of the films in powder form which were deliberately scraped from the substrates as well as on portions of the coatings which remained on the substrate. Table 11 shows a comparison of the ratio of total counts of Zn and Se recorded under the different deposition and analysis conditions. The initial comparison between the measured ratio of Zn to Se for Samples No. 7 and 8 when analyzed in powder form indicated that Sample No. 8, deposited at the higher rate, contained a higher relative amount of Zn. However, in view of the fact that large variations were noted between analyses on the powder form and those on the intact form for Sample No. 8, the apparent difference between Samples No. 7 and 8 could not confidently be considered as being real. Similar results were obtained using electron microprobe analysis. In this case, the Zn to Se signal ratio from an analysis of a piece of bulk ZnSe, the same as used as an evaporation source material was compared with that of a ZnSe coating. Table 12 displays these results. It was found that a significant effect on the results was produced when a correction to the coating data to account for

TABLE 11
X-RAY FLUORESCENCE RESULTS

<u>Sample No.</u>	<u>Deposition Rate (A/sec)</u>	<u>Sample Form</u>	<u>Zn/Se Count Ratio</u>
7	3.5	Scraped Powder	1.141
8	11	Scraped Powder	1.146
8	11	Coated Substrate	1.165*

*Corrected for substrate background effects.

TABLE 12
ELECTRON MICROPROBE RESULTS

<u>Sample</u>	<u>Zn/Se Signal Ratio</u>
Bulk ZnSe	3.29
ZnSe Coating	3.74 corrected 3.06 uncorrected

background effects from the substrate was made. Application of this correction changed the results from indicating a slight relative deficiency of Zn to indicating a somewhat larger relative excess of Zn in the coating when compared with the bulk material. Although this corrected value was felt to be more representative of the true ratio, due to the critical effect that this correction could make in data interpretation, the electron microprobe results by themselves were not interpreted as providing conclusive evidence that a deviation in coating stoichiometry existed.

Rutherford backscattering analysis (RBS) using He^{+4} ions was carried out on ZnSe coatings deposited onto CaF_2 at rates of 0.9, 6, and 80 Å/sec. The coatings ranged in thickness from 800 to 1000 Å. Within the error limits of these analyses no measurable difference was detected in the stoichiometric ratio of these coatings.

Two techniques were used to analyze the ZnSe coatings which combined surface chemical analysis with ion sputtering, thereby providing a capability for detecting changes as a function of distance through the thin film. The first of these, ESCA, was performed on two 500 Å thick coatings deposited onto CaF_2 at rates of 1 Å/sec and 20 Å/sec. Positive results of a qualitative nature were obtained from these analyses. The first result indicated that a generally higher Zn to Se ratio was evident in the coating deposited at the higher rate. A second observation which the profiling capability revealed was that stoichiometric variations were found to exist within individual ZnSe films. This was the first indication that stoichiometric differences between films could actually be the result of large but localized deviations which existed throughout the films.

The second profiling technique used was Auger electron spectroscopy (AES). For these measurements two coatings were deposited in succession on the same substrate. The first coating, 4500 Å thick, was deposited at 1 Å/sec while the second, 3000 Å thick, was deposited on top of the first at a rate of 40 Å/sec. Simultaneous depositions were made onto a glass witness plate and an Al foil substrate. The ZnSe films were deposited in two layers in an attempt to determine if the AES profiling technique could detect a change in the ratio of the Zn to Se concentration across the interface of the two films deposited at different rates. No measurable change was recorded when the measurement was made. There was noted a slight increase in the oxygen and carbon concentration at the interface, which was attributed to the fact that several minutes elapsed between the end of the first deposition and the initiation of the second. During this period, it was presumed that residual oxygen and carbon within the vacuum chamber was deposited onto the surface of the first coating. Although no detectable stoichiometric difference was observed at the

interface of the two films, a variation in stoichiometry within the films, as was noted in the ESCA analyses, was observed. This variation was found to exist in the coatings deposited on both the glass substrate and the Al foil substrate. This effect for measurements made on both substrates is shown in Figure 21. These plots show the AES results obtained during the final portion of the profile analysis performed on each of the coatings. The fact that the Zn and Se traces are at different levels in these plots does not indicate a difference in relative concentration. Rather this difference is typical of the AES measurement and only reflects a difference in the cross section for Auger electron emission between the two elements. In addition, the scale factors are different for each of the two runs preventing an absolute comparison between the two analyses. However, both of the profiles do show point to point variations in the Zn concentration which are noticeably greater than any variation in Se concentration. The simultaneous and rapid decrease in both the Zn and Se levels at the end of the analysis indicates that the film-substrate interface has been reached.

Table 13 summarizes the conclusions drawn from each of the analyses performed to determine if the Zn to Se ratio in the coatings was affected by variations in the deposition rate. As previously stated, with the possible exception of the ESCA analysis, no single technique produced irrefutable evidence that such a rate dependency existed. However, when the results of all of these analyses are combined, evidence does emerge which indicates that there is a tendency for the Zn concentration to increase at higher deposition rates. Furthermore, the ESCA and AES measurements have indicated that this concentration is not necessarily uniform throughout the ZnSe coating, but, rather, varies from point to point.

When the ESCA, AES, and electron microprobe analyses were performed to measure Zn and Se concentrations, simultaneous analyses for the presence of impurities were also included. None of these techniques were able to detect elements other than Zn or Se. Therefore, any impurities that may have been present in the ZnSe coatings existed at concentration levels which were below the sensitivity limits of these techniques.

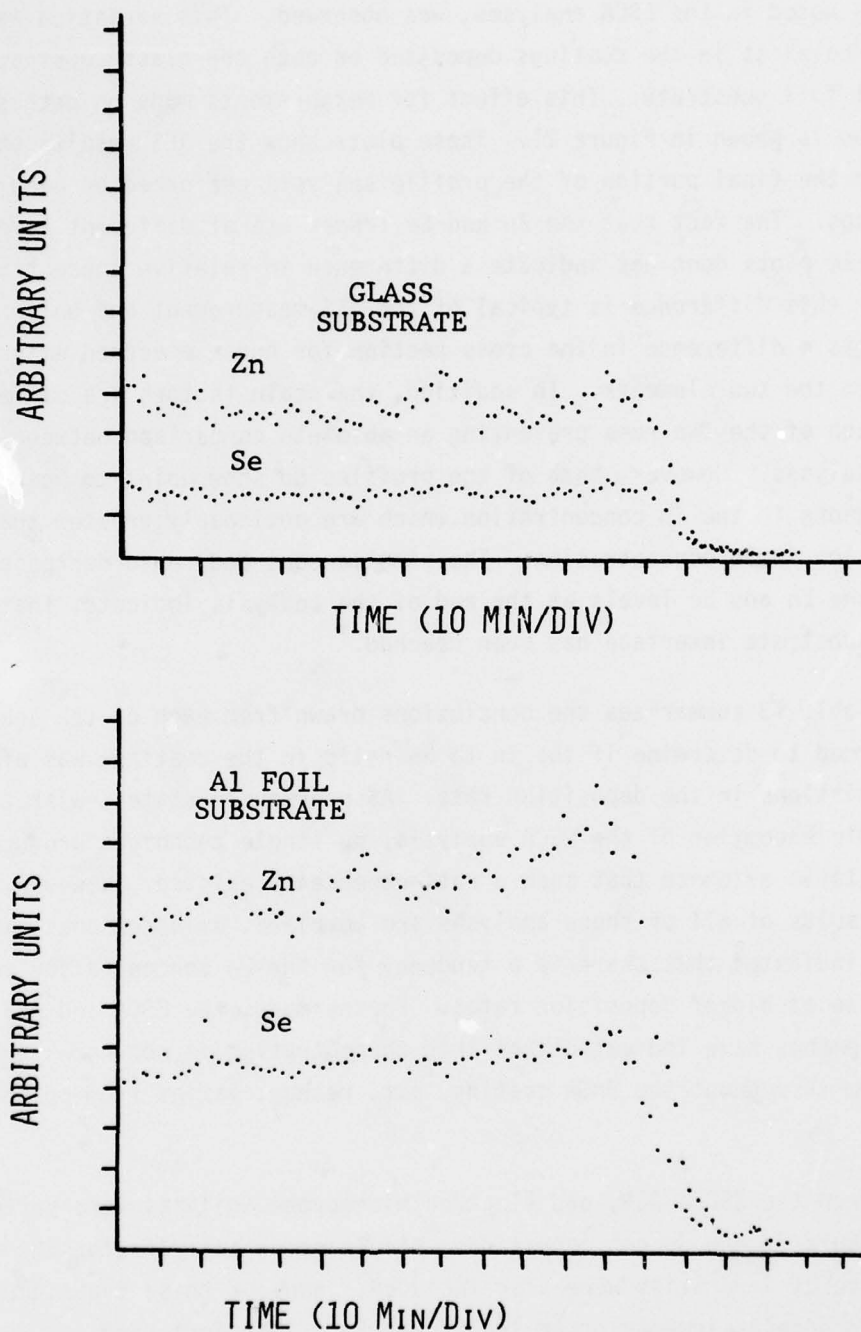


Figure 21. Auger Electron Profile Analyses of ZnSe on Glass and on Al Foil Substrates.

TABLE 13
SUMMARY OF STOICHIOMETRY ANALYSES

<u>Technique</u>	<u>Dependence of Zn to Se Ratio on Deposition Rate</u>
X-Ray Fluorescence	Possibly Higher for High Rate
Electron Microprobe	Possibly Higher for High Rate
RBS	No Dependence Detected
ESCA	Higher for High Rates; Variation Within a Single Film Noted
AES	No Dependence Detected; Variation Within a Single Film Noted

SECTION V

CONCLUSIONS AND RECOMMENDATIONS

Identification of one of the major causes for the abnormally excessive level of infrared absorption measured in ZnSe coatings has been achieved. Because of the significant difference that exists in the vapor pressures of the constituent elements, Zn and Se, a nonstoichiometric condensation of ZnSe occurs during the deposition process in which the starting material is in the compound form. This nonstoichiometry results in an increase in the Zn to Se ratio, causing a corresponding increase in the absorption of infrared radiation within the coating. The absorption of $1.06\text{ }\mu\text{m}$ laser radiation correlated to stoichiometric variations predicted by Gunther in his theoretical description of the deposition of binary compounds. Confirmation of the increased Zn to Se ratio in the coatings was indicated by the combined results of several state-of-the-art surface analysis techniques. Incorporation of the predictions based upon the theoretical model of Gunther with the experimental results obtained in this program have resulted in the identification of three controllable deposition parameters which can be used to produce a more nearly stoichiometric and hence lower absorbing ZnSe coating. The first of these parameters is deposition rate, which, it was found, should be as low as possible within the limits of reasonable total time constraints placed on the film growth. Rates of approximately $1\text{ }\text{\AA}/\text{sec}$ were the lowest used in this program, and the lowest absorption was measured in films grown at this rate. The second parameter is substrate temperature. Direct confirmation of the effect of substrate temperature on coating absorption was not possible because of the mismatch between the thermal expansion coefficients of the ZnSe coating and the CaF_2 substrate. However, based upon the fact that both Zn and Se have vaporization temperatures which are much lower than that of ZnSe and relating this fact to predictions based upon stoichiometric variations, it can be inferred that the lowest absorbing coatings will be those which are deposited onto substrates at elevated temperatures. No maximum substrate temperature can be identified, since this value depends either upon the amount of coating stress that can be tolerated or upon the

critical substrate temperature beyond which no deposition is possible. The final deposition parameter which can be used to control the coating absorption is the Zn to Se ratio in the vapor stream. By introducing an excess of Se, the more volatile element, either with an additional Se source or by separate and controllable evaporation of the two constituent elements, the resulting Zn to Se ratio in the coating can be brought closer to true stoichiometric proportions. The optimum ratio to be used is dependent upon both the substrate temperature and the flux rate, as demonstrated by Gunther in his investigations of CdSe film growth. Identification of the relationship of these three parameters for the particular case resulting in the optimal growth of ZnSe was not attempted in this program, due to the lack of the unique equipment and instrumentation such a determination requires. However, the need for such an investigation is certainly recognized and it is recommended that additional programs which address this problem be pursued if possible.

Although an excess of Zn was determined to be the primary cause for the increased infrared absorption in ZnSe coatings, the exact nature of how this excess Zn occurs within the compound was not identified. Results of growth studies of related II-VI compounds have shown that interstitial atoms or inclusions of the less volatile constituent occur as well as voids or vacancies of the more volatile element. However, the overall result of any of these conditions is usually a deviation in the stoichiometric ratio of the constituents, which indicates an excess of the less volatile component. The results of ESCA and AES profile analyses revealed that the nonstoichiometry of the ZnSe thin films is not uniform throughout the film, but rather occurs as localized deviations which, however, on a macroscopic level appear as a uniform effect. Although this result was not predicted by the Gunther model, it in no way conflicts with any of its interpretations.

Another significant conclusion which was drawn from the results of this research effort is that the major portion of the high film absorption occurs within the bulk of the ZnSe film and not at the surface or interface. Similarly, it was found that the presence of impurities has not been a principal cause for the very large absorption levels measured

in these coatings. However, it is quite possible that with improvements in the ability to grow stoichiometric ZnSe films, these sources of absorption could take on more importance.

Since the total fractional absorption within state-of-the-art infrared materials used as coating substrates is on the order of 1×10^{-4} , calorimetry measurements on thin films which display absorption levels below this value tend to be somewhat unreliable. For a $1 \mu\text{m}$ thick coating this limiting value represents an effective absorption coefficient of 1 cm^{-1} , a value slightly below the lowest measured in this program. Although the absorption coefficient of bulk ZnSe is still more than two orders of magnitude lower than this, further attempts at investigating additional means of decreasing coating absorption to these levels becomes very difficult because of calorimeter limitations. The results of this research, however, have indicated that although stoichiometric variations significantly affect absorption occurring within the ZnSe coatings, other unspecified mechanisms also affect absorption to a somewhat lesser degree. Some of these mechanisms are included in Table 2, and it is these areas which must next be considered if further improvements are to be attained. Some of these areas are already being addressed, as indicated by recently initiated programs to improve the purity of evaporation source materials (Reference 54) and to investigate the uses of ultra-high vacuum technology in coating depositions (Reference 55). Further decreases in absorption within coatings, if achieved by these programs, will ultimately lead to a situation where research into the causes of residual absorption will be greatly hindered due to the lack of an analytical capability to detect this absorption. Thus, a final recommendation emerging from this study indicates the definite need to develop new and additional analytical techniques to satisfy these measurement requirements.

BIBLIOGRAPHY

1. Loomis, J.S., Antireflection Coating Designs for 10.6 - Micron Window Materials. AFWL-TR 72-180 Air Force Weapons Laboratory, Kirtland AFB, NM (1973).
2. Pastor, R.C., and Braunstein, M., Halide Window Materials Technology. AFWL-TR-72-38 Air Force Weapons Laboratory, Kirtland AFB, NM (1972).
3. Kurdock, J.R., Optical Properties of Alkali Halides and Zinc Selenide for High Power Laser Applications. AFML-TR-74-166 Air Force Materials Laboratory, Wright-Patterson AFB, OH (1975).
4. Braunstein, M., and Rudisill, J.E., Protective-Antireflective Thin Films for Polycrystalline Zinc Selenide and Alkali Halide Laser Windows. AFML-TR-75-18 Air Force Materials Laboratory, Wright-Patterson AFB, OH (1975).
5. Braunstein, M., et al., "Low Absorption Antireflection Coatings for KCl," in Proceedings of the Fifth Annual Conference on Infrared Laser Window Materials. C.R. Andrews and C.L. Strecker, eds. Defense Advanced Research Projects Agency, Arlington, VA (1976).
6. Shiozawa, L.R., et al., The Application of Physical Vapor Deposition to Semiconductor Materials for Use as High Power Infrared Windows. AFML-TR-73-163, Air Force Materials Laboratory, Wright-Patterson AFB, OH (1973).
7. Swanson, A.W., and Pappis, J., Application of Polycrystalline ZnSe Prepared by Chemical Vapor Deposition to High Power IR Laser Windows. AFML-TR-75-170, Air Force Materials Laboratory, Wright-Patterson AFB, OH (1975).
8. Sahagian, C.S., and Pitha, C.A. eds., Conference on High Power Infrared Laser Window Materials, 1971. AFCRL-TR-71-0592, Air Force Cambridge Research Laboratories, L.G. Hanscom Field, Bedford, MA (1971).
9. Pitha, A., ed., Conference on High Power Laser Window Materials, 1972. AFCRL-TR-73-0372 Air Force Cambridge Research Laboratories, L.G. Hanscom Field, Bedford, MA (1972).
10. Pith, C.A., et al., eds., Third Conference on High Power Laser Window Materials, 1973. AFCRL-TR-74-0085 Air Force Cambridge Research Laboratories, L.G. Hanscom Field, Bedford, MA (1974).
11. Andrews, C.R., and Strecker, C.L., eds., Proceedings of the Fourth Annual Conference on Infrared Laser Window Materials. Defense Advanced Research Projects Agency, Arlington, VA (1975).
12. Andrews, C.R., and Strecker, C.L., eds., Proceedings of the Fifth Annual Conference on Infrared Laser Window Materials. Defense Advanced Research Projects Agency, Arlington, VA (1976).

BIBLIOGRAPHY (CONTINUED)

13. Andrews, C.R., and Strecker, C.L., eds., Proceedings of the Sixth Annual Conference on Infrared Laser Window Materials. Defense Advanced Research Projects Agency, Arlington, VA (1976).
14. Harris, J., and Strecker, C.L., eds., Proceedings of the High Power Laser Optical Components and Component Materials Symposium, Oct 1977. Defense Advanced Research Projects Agency, Arlington, VA (1978).
15. Mitra, S.S., and Bendow, B., eds., Optical Properties of Highly Transparent Solids. Plenum Press, New York (1975).
16. Rowe, J.M., and Harrington, J.A., "Multiphonon Absorption in KCl, NaCl, and ZnSe," in Ref. 14, 109-118.
17. Winsor, H.V., "The Role of Scattering in Calorimetric Measurements of Infrared Absorption Coefficients," in Ref. 8, 351-368.
18. Holland, L., Vacuum Deposition of Thin Films. Chapman and Hill, Ltd., London (1970), 294-297.
19. Snedjar, D., et al., "Electrical Conduction Mechanism in CdSe Films Prepared by Vacuum Evaporation and Annealed in Se Vapor," in Thin Solid Films 9, 97-107 (1971).
20. Glang, R., et al., "Vacuum Evaporation of Cadmium Telluride," in Journal of the Electrochemical Society. 110, 407-412 (May 1963).
21. Moore, R.M., et al., "Vacuum-Deposited CdSe Films Grown Under Excess Se Flux," in Thin Solid Films 26, 363-370 (1975).
22. Foster, N.F., "Structure of CdS Films in Relation to Their Use as Ultrasonic Transducers," in Journal of Applied Physics 38, 149-159 (Jan 1967).
23. -----, Development of Low Cost Hardened Zinc Selenide for IR Windows. Monthly Letter Reports No. 4 and No. 10, Air Force Contract No. F33-615-75-C-5131, Air Force Materials Laboratory, Wright-Patterson AFB, OH.
24. Bowen, K.H., and VanderSande, J., Chemical Vapor Deposition of Chalcogenide Semiconductors. AFML-TR-75-91 Air Force Materials Laboratory, Wright-Patterson AFB, OH (1975).
25. Gunther, Karl-Georg, "Interfacial and Condensation Processes Occurring with Multicomponent Vapors," in The Use of Thin Films in Physical Investigations. J.C. Andrews ed., Academic Press, New York (1966).

BIBLIOGRAPHY (CONTINUED)

26. Sparks, M., Theoretical Studies of High-Power Infrared Window Materials. Final Technical Report December 1972, ARPA Order No. 1969-Program Code No. 2D10 (1972), pp. 90-110.
27. Yarovaya, R.G., et al., "Temperature Dependence of the Optical Properties and the Energy Spectrum of Zinc," in Soviet Physics - JETP 38, 331-334 (Feb 1972).
28. Feldman, A., et al., "Optical Properties of Polycrystalline Zinc Selenide," in Ref. 11, 118-129.
29. Wooten, F., Optical Properties of Solids. Academic Press, New York (1972), p. 58.
30. Braunstein, M., and Rudisill, J.E., Protective Antireflective Thin Films for Polycrystalline Zinc Selenide and Alkali Halide Laser Windows. AFML-TR-75-18 Air Force Materials Laboratory, Wright-Patterson AFB, OH (1975).
31. Braunstein, M., et al., Laser Window Surface Finishing and Coating Science. AFCRL-TR-76-0048 Air Force Cambridge Research Laboratories, L.G. Hanscom Field, Bedford, MA (1976).
32. Weil, R., "Calculation of Small Optical Absorption Coefficients from Calorimetric Experimental Data," in Journal of Applied Physics 41, 3012-3014 (Jun 1970).
33. Loomis, J.S., "Absorption in Coated Laser Windows," in Applied Optics 12, 877-878 (Apr 1973).
34. Silver, M.D., and Chow, T.K., "Thickness Measurements of Thin Permalloy Films Comparison of X-Ray Emission Spectroscopy, Interferometry, and Stylus Methods," in Journal of Vacuum Science and Technology 2, 203-207 (Jan/Feb 1965).
35. Breitweiser, G., "Surface Profile Measurement - A Survey of Applications in the Area of Vacuum Deposition," in Journal of Vacuum Science and Technology 11, 11-15 (Jan/Feb 1974).
36. Heavens, O.S., Optical Properties of Thin Solid Films. Dover Publications, Inc., New York (1965), pp. 96-154.
37. McCrackin, F., A Fortran Program for Analysis of Ellipsometer Measurements. National Bureau of Standards Technical Note 479, U.S. Government Printing Office, Washington (1969).
38. Heavens, O.S., "Measurement of the Optical Constants of Thin Films," in Physics of Thin Films Vol. 2, George Hass, ed. Academic Press, New York (1964).

BIBLIOGRAPHY (CONTINUED)

39. Soleau, M.J., et al., "Polishing Studies and Backscatter Measurements on Alkali-Halide Windows," in Laser Induced Damage in Optical Materials: 1975. NBS Special Publication 435, A. Glass and A. Gunther eds. (Apr 1976).
40. Kane, P.F., and Larabee, G.R., eds., Characterization of Solid Surfaces. Plenum Press, New York (1974).
41. Mayer, J.W., and Ziegler, J.F., eds., Ion Beam Surface Layer Analysis. Proceedings of the Third International Conference held on June 18-20, 1973, Yorktown Heights, New York; American Elsevier Publishing Co. Inc., New York (1974).
42. Evans, C.A., Jr., "Surface and Thin Film Compositional Analysis," in Analytical Chemistry 47, 818A-828A (Aug 1975).
43. Hutchins, G.H., "Electron Probe Microanalysis," in Ref. 53, 441-484.
44. Gilfrich, J.V., "X-ray Fluorescence Analysis," in Ref. 39, 275-306.
45. Newberg, R.T., and Pappis, J., Casting of Halide and Fluoride Alloys for Laser Windows. AFCRL-TR-76-0011 Air Force Cambridge Research Laboratories, L.G. Hanscom Field, Bedford, MA (1976), pp. 83-91.
46. Dickinson, S.K., Infrared Laser Window Materials Property Data for ZnSe, KCl, NaCl, SrF₂, BaF₂. AFCRL-TR-75-0318 Air Force Cambridge Research Laboratories, L.G. Hanscom Field, Bedford, MA (1975).
47. Moses, A.J., Handbook of Electronic Materials Volume 1 Optical Material Properties. IFI/Plenum Data Corp., New York (1971), p. 32.
48. Yim, W.M., and Stafko, E.J., "Vapor-Phase Epitaxial Growth and Some Properties of ZnSe, ZnS, and CdS," in Journal of the Electrochemical Society: Solid State Science and Technology 119, 381-388 (Mar 1972).
49. Detrio, J.A., et al., Optical Evaluation and Characterization of IR Transmitting and Laser Window Materials. UDRI-TR-76-39 University of Dayton Research Institute, Dayton, OH (1976).
50. Johnston, G.T., et al., Laboratory Characterization and Research on the Performance of Window Materials for High Power IR Lasers. AFML-TR-73-214, Air Force Materials Laboratory, Wright-Patterson AFB, OH (1973).
51. Willingham, C.B., "Laser Calorimetry of Infrared Optical Thin Films," in Ref. 12, 356.

BIBLIOGRAPHY (CONCLUDED)

52. Rosenstock, H.B., "Infrared Bulk and Surface Absorption," in Ref. 12, 860.
53. Shiozawa, L.R., and Jost, J.M., Research on Improved II-VI Crystals. ARL 71-0017 Aerospace Research Laboratories, Wright-Patterson AFB, OH (1971).
54. Swenson, O.F., Private communication.
55. , Ultra Low Loss Coatings for Potassium Chloride Laser Windows. Air Force Contract No. F33-615-76-C-5319, Air Force Materials Laboratory, Wright-Patterson AFB, OH.
56. Miles, P.A., Research on Halide Superalloy Windows. AFCRL-TR-73-0758, Air Force Cambridge Research Laboratories, L.G. Hanscom Field, Bedford, MA (1973), pp. 4-69.